were monitored using flow cytometric analysis with rhodamine 123 staining. C26 cells (1.0×10^6 cells/well) were cultured in six-well plates for 12 h, washed twice with PBS, and incubated with PBS and either 100 μM HSA or various concentrations of NO-HSA in medium A for 24 h. The cells were then trypsinized, washed twice with PBS, and incubated for 15 min with 5 μg/ml rhodamine 123. The mean fluorescence intensity of rhodamine 123 in the cells was measured using a flow cytometer (FACSCalibur; BD Biosciences, Franklin Lakes, NJ).

For the determination of caspase-3 activity, cells were cultured to confluence in six-well plates, washed twice with PBS, and incubated with medium A containing 100 μM HSA or various concentrations of NO-HSA. Cells were incubated for 24 h, trypsinized, and washed with 0.2 ml of ice-cold PBS. The cell pellet was resuspended in 15 μl of cell lysis buffer, it was lysed by freeze-thawing, and then it was incubated on ice for 15 min. The cell lysates were centrifuged at 15,000 rpm for 20 min at 4°C, and the supernatant fraction was collected (cell extract). The caspase-3 activity in the cell extract was assessed using the colorimetric CaspASE Assay System (Promega, Madison, WI), according to the manufacturer's instructions.

For the detection of DNA degradation (DNA ladder), C26 cells (1.0×10^6 cell/well) were cultured in six-well plates. Cells were cultured for 12 h, they were washed twice with PBS, and then they were incubated with PBS and either 100 μM HSA or various concentrations of NO-HSA for 24 h. The cells then were trypsinized, collected, and centrifuged at 4000 rpm for 10 min. After removing the supernatant, the cell pellet was resuspended in 0.2 ml of PBS, and then it was centrifuged at 4000 rpm for 10 min. The supernatant was again removed, and the remaining pellet was incubated in 20 μl of 10 mM Tris-HCl buffer, pH 7.8, containing 2 mM EDTA and 0.5% SDS (cell lysis buffer) for 10 min at 4°C, followed by centrifugation at 15,000 rpm for 5 min. The resulting supernatant (cell extract) was collected and incubated with 1 μl of RNase A (10 μg/ml) for 30 min at 50°C. One microliter of proteinase K (10 μg/ml) was added to the cell extract, followed by a 1-h incubation at 50°C. The resulting DNA extract was electrophoresed in a 2.0% agarose gel, followed by staining of the gel with ethidium bromide and visualization of the DNA bands using ultraviolet illumination.

The cell viability assay was performed using WST-8, which is based on the 3-(4,5-dimethylthiazol-2-yl)-2,5-diphenyltetrazolium assay. C26 cells were plated in 96-well plates at 1.0×10^4 cells/well, and they were cultured for 32 h in medium A. Then, the cells were washed twice with PBS and incubated in a total volume of 0.2 ml of medium A containing various concentrations of HSA or NO-HSA. After incubating the cultures for various lengths of time, 5 μl of WST-8 solution was added to each well, and the cells were incubated for an additional 2 h at 37°C. The number of surviving cells was determined by measuring the absorbance at 450 nm. Cell viability was calculated as the percentage of the control value (without HSA or NO-HSA) (Ishiyama et al., 1996).

Animal Experiments. Five-week-old male BALB/c AnNCrlCrlj mice (17–20 g) were purchased from Charles River Italica (Calco, Italy). The mice were housed in a 12-h light/dark cycle in a humidity-controlled room. Mice were acclimated for at least 5 days before being used in experiments.

For tumor induction, mice were inoculated with C26 cells (1.0×10^6 cells/mouse) by a subcutaneous injection into the dorsal skin. Three days after inoculation, C26 carcinoma-bearing mice were randomly divided into three groups: control, HSA, and NO-HSA. The mice received a daily i.v. injection of saline, HSA (10 μmol/kg), or NO-HSA (10 μmol/kg) for 10 days from day 3 to day 12 after inoculation. Tumor volume was calculated using the formula $0.4\ (a \times b^2)$, where a is the largest diameter and b is the smallest diameter of the tumor (Shimizu et al., 2005), and volume was monitored from day 7 to day 17 after inoculation. Variance in each group was evaluated using the Bartlett test, and differences in mean tumor volume were evaluated using the Tukey-Kramer test.

Some animals in each of the three treatment groups were used for immunohistochemical analysis and serum biochemistry. When the mice received five times per day from day 3 to day 7 after inoculation (the tumors in each group reached approximately 5 mm in diameter), blood samples were collected from the abdominal vena cava under diethyl ether anesthesia approximately 2 h after the daily injection, and then the mice were sacrificed.

Tumors were dissected, they were fixed immediately with 2% periodate/lysine/paraform-aldehyde fixative at 4°C for 5 h, and then they were washed with a graded series of sucrose solutions in PBS (10, 15, and 20%). After immersion in 20% sucrose in PBS to inhibit ice crystal formation, the tissues were embedded in O.C.T. compound (Sakura Fine Technochemical, Tokyo, Japan), they were frozen in liquid nitrogen, and then they were stored at −80°C. Five-micrometer tumor sections were prepared using a cryostatic microtome (HM500M; Microm, Walldorf, Germany), and they were mounted on poly-L-lysine-coated slides. The slides were stained using the TUNEL method and an in situ apoptosis detection kit (Takara-Bio Co. Ltd., Shiga, Japan). The slides were washed three times with 0.01 M phosphate buffer, pH 7.4, containing 0.9% NaCl, followed by application of methanol containing 0.3% H_2O_2 to inactivate endogenous peroxidase and incubation at room temperature for 30 min. The slides were washed 3 times with 0.01 M phosphate-buffered saline, and then they were incubated in 100 ml of permeabilization buffer on ice for 5 min. The slides were washed three times with 0.01 M phosphate-buffered saline, and then they were incubated with 50 ml of freshly prepared terminal deoxynucleotidyl transferase reaction mixture (5 ml of terminal deoxynucleotidyl transferase enzyme + 45 ml of Labeling Safe buffer) at 37°C for 60 min. After the slides were washed three times with 0.01 M PBS, they were incubated in 70 ml of anti-fluorescein isothiocyanate-horseradish peroxidase conjugate antibody at 37°C for 30 min. After the slides were washed three times with 0.01 M PBS, they were incubated in 3,3-diaminobenzidine-H_2O_2 reaction buffer at room temperature for 10 min. After the slides were washed three times with distilled water, they were stained with 3% methyl green for 10 min, dehydrated, penetrated, and sealed (Gavrieli et al., 1992). Each slide then was visualized under a light microscope (Olympus, Tokyo, Japan), at a magnification of 400×.

Serum was separated by centrifugation. Routine clinical laboratory techniques were used to determine the concentrations of total protein, serum creatinine (Cr), blood urea nitrogen (BUN), alanine aminotransferase (ALT), aspartate aminotransferase (AST), and alkaline phosphatase (ALP) in serum. Variance in each group was evaluated using the Bartlett test, and differences were evaluated using the Tukey-Kramer test.

Results

NO-HSA Induces Cell Death via Apoptosis in Vitro. Apoptosis is induced by a variety of factors. Among them, it is well known that intracellular accumulation of ROS, such as H_2O_2, O_2^-, and peroxynitrite, causes apoptosis. Moreover, production of ROS also plays a major role in NO-ASA-induced apoptosis. To examine whether NO-HSA promoted ROS production in C26 cells, a fluorescent probe (CM-H_2DCFDA), which undergoes conversion to 2′,7′-dichlorofluorescein in the presence of intracellular ROS, was used. Addition of NO-HSA to C26 cells increased the amount of ROS compared with treatment with vehicle or HSA (Fig. 2). In addition, the ROS in the C26 cell culture medium increased with time after addition of NO-HSA. This result suggests that NO-HSA promotes a signal cascade leading to apoptosis by increasing intracellular production of ROS.

To evaluate the effect of NO-HSA on mitochondrial function, C26 cells were loaded with a mitochondria-selective fluorescent cation (rhodamine 123) to monitor the mitochon-

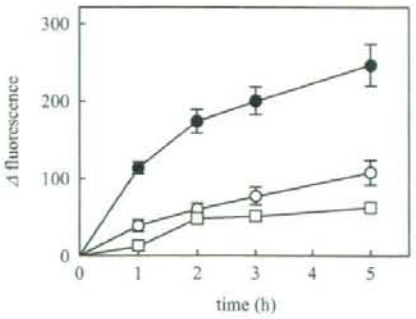

Fig. 2. Production of ROS in C26 cells after NO-HSA treatment. C26 cells were pretreated with CM-H_2DCFDA for uptake into C26 cells and hydrolysis by cellular esterase, followed by addition of either PBS (open circles), 50 μM HSA (open squares), or 50 μM NO-HSA (closed circles). Excitation of the probes was done at 485 nm, and emission was measured at 535 nm. Change in fluorescence was calculated by subtracting the fluorescence at 0 h from that at the indicated times. The fluorescence intensities of the PBS, 50 μM HSA, and 50 μM NO-HSA groups at 0 h were 201.3, 166.1, and 181.3, respectively. Results are the mean ± S.D. of three separate experiments.

drial membrane potential. Compared with vehicle, in cells treated with 50 or 100 μM NO-HSA rhodamine 123, fluorescence was decreased by 75%, whereas treatment with 25 μM NO-HSA or 100 μM HSA did not affect rhodamine 123 fluorescence compared with vehicle (Fig. 3A). These observations indicate that NO-HSA induces depolarization of the mitochondrial membrane.

Caspase-3 is a cell death protease that is involved in the downstream execution phase of apoptosis. During this phase of apoptosis, cells undergo morphological changes, such as DNA fragmentation, chromatin condensation, and formation of apoptotic bodies. Compared with the effect of vehicle, cells treated with 25 or 50 μM NO-HSA had slightly increased caspase-3 activity, and cells treated with 100 μM NO-HSA showed a larger increase in caspase-3 activity (Fig. 3B). Cells treated with HSA had the same level of caspase-3 activity as cells treated with PBS.

To further confirm that NO-HSA induced apoptosis in C26 cells, DNA fragmentation, which is a typical morphological change in the execution phase of apoptosis, was examined. DNA fragmentation was observed in C26 cells treated with 100 μM NO-HSA, but not in C26 cells treated with 25 or 50 μM NO-HSA (Fig. 3C). Neither vehicle nor 100 μM HSA induced DNA fragmentation in C26 cells (Fig. 3C). These findings suggest that NO-HSA induces apoptosis by increasing ROS production, activating caspase-3, and hyperpolarizing the mitochondrial membrane potential.

To determine the effect of NO-HSA on cell growth, the viability of C26 cells was examined after treatment with HSA or various concentrations of NO-HSA. NO-HSA inhibited growth of C26 cells in a concentration-dependent manner; cell growth was suppressed by 71, 80, and 85% after a 48-h incubation with 25, 50, and 100 μM NO-HSA, respectively (Fig. 4A). The viability of C26 cells incubated with 50 μM NO-HSA significantly decreased with increasing incubation times (Fig. 4B). NO-HSA inhibited growth to a greater extent than did HSA, which had only a weak inhibitory effect. These results suggest that NO-HSA inhibits cell growth of C26 cells by inducing apoptosis.

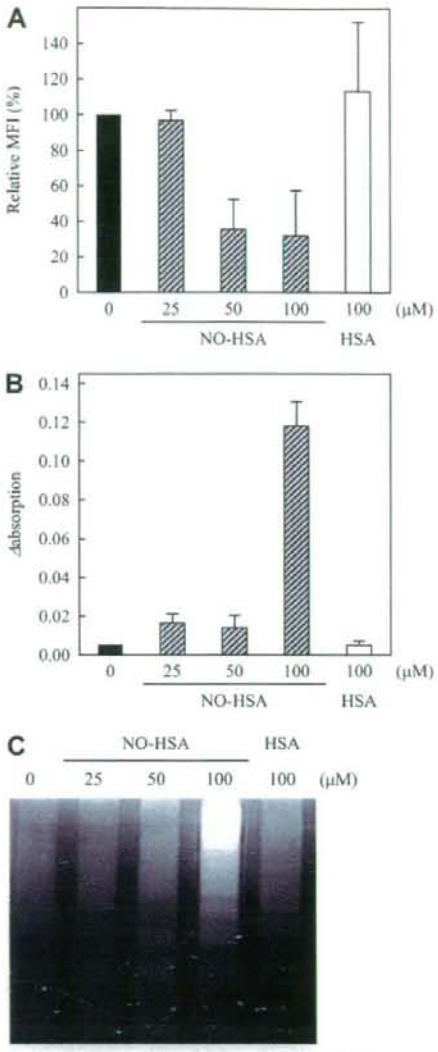

Fig. 3. Induction of apoptosis of C26 cells after NO-HSA treatment. A, alteration in the mitochondrial membrane potential after NO-HSA treatment. C26 cells were cultured with PBS, 100 μM HSA, or various concentrations of NO-HSA for 24 h, followed by addition of rhodamine 123. The amounts of cell-associated rhodamine 123 were determined as described under *Materials and Methods*. Results are the mean ± S.D. of three separate experiments. B, activation of caspase-3 after NO-HSA treatment. C26 cells were incubated with PBS, 100 μM HSA, or various concentrations of NO-HSA for 24 h. Caspase-3 activity was estimated by monitoring *p*-nitroaniline (absorbance at 405 nm) released from the substrate upon cleavage by caspase-3. Change in absorbance was calculated by subtracting absorbance after incubation with caspase inhibitor (*N*-benzyloxycarbonyl-Val-Ala-Asp-fluoromethylketone), from absorbance after incubation without caspase inhibitor. The absorbances among PBS-, HSA- and NO-HSA-treated cells incubated with *N*-benzyloxycarbonyl-Val-Ala-Asp-fluoromethylketone were almost identical (0.170 ± 0.17). Results are the means ± S.D. of three separate experiments. C, DNA fragmentation after NO-HSA treatment. C26 cells were incubated with PBS, 100 μM HSA or various concentrations of NO-HSA for 24 h. DNA fragmentation was detected as described under *Materials and Methods*.

NO-HSA Exerts Antitumor Effect via the Apoptotic Pathway in Vivo. To investigate the antitumor effect of NO-HSA in vivo, C26 tumor-bearing mice received i.v. injec-

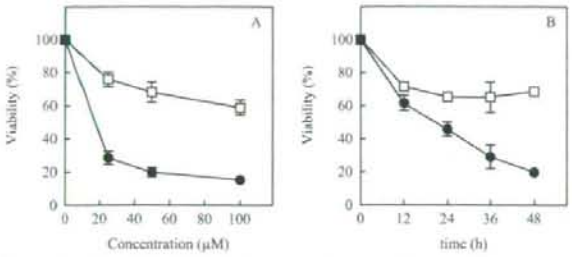

Fig. 4. Effect of NO-HSA on C26 cell viability. A, C26 cells were treated for 48 h with various concentrations of HSA (open squares) or NO-HSA (closed circles). B, C26 cells were incubated for the indicated times with 100 μM HSA (open squares) or 100 μM NO-HSA (closed circles). Cell viability was determined as described under *Materials and Methods*. Results are the mean ± S.D. of three separate experiments.

tions with saline, HSA, or NO-HSA. Mean tumor area increased with time in the saline-treated group. In the HSA-treated group, tumor growth was suppressed, compared with that in the control group, but the difference was not statistically significant. In contrast, tumor growth was significantly inhibited by administration of NO-HSA (Fig. 5).

To clarify whether the suppression of tumor growth by NO-HSA is mediated via apoptosis, tumor tissues from C26 tumor-bearing mice receiving injections with NO-HSA were examined using immunohistochemistry. In NO-HSA-treated mice, there were more TUNEL-positive cells than in the saline- and HSA-treated animals. In addition, the tumor tissue architecture was less defined in animals treated with NO-HSA than in the other groups, suggesting that NO-HSA induced apoptosis in C26 tumor cells and thus exerted an antitumor effect in vivo (Fig. 6).

To evaluate the side effects of NO-HSA treatment, several serum biochemical parameters were measured in tumor-bearing mice treated with saline, HSA, or NO-HSA (Table 1). There were no significant differences in total protein, Cr, BUN, AST, or ALT among the three groups, suggesting that

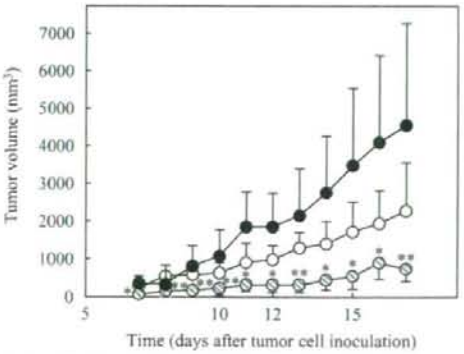

Fig. 5. Effect of NO-HSA on tumor growth in C26 tumor-bearing mice. C26 tumor-bearing mice were given daily i.v. injections of saline (5 ml/kg), HSA (10 μmol/5 ml/kg), or NO-HSA (10 μmol/5 ml/kg) for 10 days from day 3 to day 12 after inoculation with tumor cells. Tumor size was measured and tumor volume was calculated according to the formula: $V = 0.4a^2b$, where a is the smallest, and b is the largest, superficial diameter. Results are means ± S.D; $n = 10$ animals per experimental group. *, statistically significant reduction compared with saline ($P < 0.01$) or HSA ($P < 0.05$) at the corresponding time. **, statistically significant reduction compared with saline ($P < 0.01$) or HSA ($P < 0.01$) at the corresponding time.

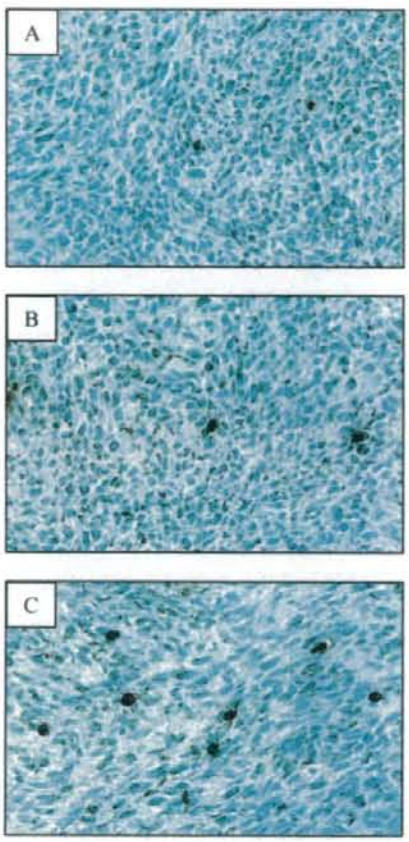

Fig. 6. Immunohistochemical staining of tumor tissues of C26 tumor-bearing mice receiving i.v. injections with NO-HSA using the TUNEL method. C26 tumor-bearing mice were given daily i.v. injections of saline (5 ml/kg) (A), HSA (10 μmol/5 ml/kg) (B), or NO-HSA (10 μmol/5 ml/kg) (C) for 5 days from day 3 to day 7 after inoculation with tumor cells. TUNEL staining, performed as described under *Materials and Methods*, shows apoptotic cells in the tumor tissue of mice treated with NO-HSA.

TABLE 1

Serum biochemical parameters of C26 tumor-bearing mice treated with saline, HSA, or NO-HSA

C26 tumor-bearing mice received i.v. injections five times per day with saline (5 ml/kg), HSA (10 μmol/5 ml/kg), or NO-HSA (10 μmol/5 ml/kg) from day 3 to day 7 after inoculation with tumor cells. Blood samples were collected from the abdominal vena cava under anesthesia with diethyl ether approximately 2 h after the last treatment injection, and mice were sacrificed. Serum biochemical parameters were measured using routine clinical laboratory techniques.

Serum Biochemical Parameter	Saline	HSA	NO-HSA
Total protein (g/dl)	5.23 ± 0.21	5.33 ± 0.06	5.55 ± 0.24
Cr (mg/dl)	0.13 ± 0.04	0.14 ± 0.01	0.16 ± 0.01
BUN (mg/dl)	15.25 ± 0.96	15.33 ± 1.53	13.75 ± 1.26
AST (U/l)	143.5 ± 62.9	91.7 ± 39.4	116.3 ± 69.1
ALT (U/l)	169.8 ± 111.6	110.0 ± 81.2	161.3 ± 126.2
ALP (U/l)	385.3 ± 18.3	345.3 ± 4.7*	300.5 ± 23.0**,†

* $P < 0.05$, saline vs. HSA.
** $P < 0.01$, saline vs. NO-HSA.
† $P < 0.05$, HSA vs. NO-HSA.

NO-HSA did not cause kidney or liver damage. However, compared with the control group, mice treated with HSA had significantly lower serum levels of ALP (345.3 ± 4.7 versus 385.3 ± 18.3 U/l). Moreover, the serum concentration of ALP

in mice treated with NO-HSA was 300.5 ± 23.0 U/l, which was significantly lower than the control ($P < 0.01$) and HSA ($P < 0.05$) groups. In general, ALP levels increase in several types of cancer, such as liver, lung, and bone cancer; thus, the present findings suggest that NO-HSA is an effective anticancer agent. The vasodilating effect of NO-HSA was also evaluated in rats after i.v. injection at a dose of 10 μmol/kg (66 μmol of NO per kg). NO-HSA induced a decrease in the mean arterial blood pressure immediately after i.v. injection and the maximum reduction effect was 32.8 ± 7.3 mm Hg. In contrast, HSA had no significant effect on the blood pressure. The fall in pressure returned to the initial levels in 30 min (data not shown).

Discussion

There have been many trials of NO as a therapeutic agent, because of its powerful biological activity (Moncada and Higgs, 1993). However, the in vivo half-life of NO (~0.1 s) is often too short to capitalize on its potential biological actions. The half-life of NO can be prolonged by adding *S*-nitrosothiol moieties with cysteine residues of proteins. For example, nitrosated HSA seems to act as a reservoir of NO in vivo (Stamler et al., 1992). Simon et al. (1996) incubated bovine serum albumin (BSA) with 200-fold excess concentration of $NaNO_2$ under acidic condition to synthesize polynitrosylated BSA that is highly modified at the thiol group of cysteine, hydroxyl group of tyrosine and amines (38 mol NO/mol BSA). The polynitrosylated BSA has been shown to exhibit antiplatelet activity. However, polynitrosylated *S*-NO-BSA, an NO-BSA conjugate prepared with the same method except that the BSA has been reduced with dithiothreitol and it contains 19 mol of "*S*-NO" per mol of BSA, was a significantly more potent platelet inhibitor than polynitrosylated BSA described above. These findings show that nitrosylated BSA behaves as an NO donor; in particular, the poly(*S*-nitroso) derivative could be by far the most potent compound. One molecule of HSA contains 35 cysteine residues, 34 of which form 17 nonreactive disulfide bonds, and one of which (Cys-34) forms a reactive free thiol (Peters, 1985). Thus, the number of NO molecules that can be bound to HSA is limited because only one free cysteine per HSA molecule is available for conjugation. Ewing et al. increased the number of free sulfhydryl groups on BSA by reduction with dithiothreitol and thiolation with *N*-acetylhomocysteine, thereby preparing polynitrosated BSA (12–15 mol NO/mol BSA) (Ewing et al., 1997). Marks et al. (1995) produced polynitrosated BSA (5.9 mol NO/mol BSA) by adding free sulfhydryl groups to the molecule and by treating the BSA with *N*-acetylhomocysteine thiolactone. However, the polynitrosated BSAs prepared in these studies formed aggregates as a result of intermolecular disulfide formation. Aggregate formation results in molecular heterogeneity, which limits the therapeutic application of *S*-nitroso residues. In the present study, iminothiolane, which reacts with primary amines to introduce sulfhydryl groups while maintaining charge properties similar to the original amino groups, was selected as the thiolation reagent. Iminothiolane was used to produce polynitrosated HSA (NO-HSA) (6.6 mol NO/mol HSA), which did not form aggregates after nonreducing SDS-PAGE or native-PAGE (data not shown). Moreover, the far-UV CD spectra of NO-HSA were nearly identical to those of HSA (data not shown). Therefore, NO-HSA is expected to be clinically applicable as a biocompatible pharmacological agent, although further study is required to clarify other potential issues, including the antigenicity of this protein.

NO-NSAIDs have been extensively investigated as therapeutic agents for cancer due to their ability to release NO, thereby promoting apoptosis. NO-NSAIDs are categorized as organic nitrate esters, which are readily reduced to organic nitrite esters by cytosolic enzymes. Subsequently, glutathione reacts with organic nitrite esters to form GSNO, indicating that NO-NSAIDs release NO via *S*-nitrosothiol (Wong and Fukuto, 1999). Alternatively, the transfer of NO from NO-HSA to the cytosol could be inferred from a study by Ramachandran et al. (2001). They reported that NO is released from extracellular *S*-nitrosothiols by a cell surface enzyme (protein disulfide isomerase) and that it accumulates in the cell membrane where it reacts with O_2 to produce N_2O_3, which is then available for nitrosation reactions with intracellular thiols at the membrane-cytosol interface (Ramachardran et al., 2001). Therefore, it is possible that NO-HSA also releases NO by the intracellular formation of *S*-nitrosothiol, suggesting that the species of NO released within the cell by *S*-nitrosothiols, as well as the reactive substances (such as ROS) derived from the released NO, would not differ significantly between NO-NSAIDs and NO-HSA. In support of this hypothesis, NO-HSA caused depolarization of the mitochondrial membrane potential, activation of caspase-3 and DNA fragmentation in the present study, consistent with the effects of NO-NSAIDs. Additional studies are needed to determine the details of the molecular events and the systematic pathways affected by NO-HSA, but the mechanism of action should be similar to that of NO-NSAIDs. In a recent study, Gao et al. (2005) elucidated the detailed mechanism of apoptosis induced by NO-ASA. Intracellular accumulation of ROS is a key proximal event in NO-ASA-induced apoptosis, and it correlates with the effect on tumor cell growth (Gao et al., 2005). In the present study, NO-HSA induced accumulation of ROS in tumor cells, suggesting that increased ROS production may be an important proximal event leading to induction of apoptosis.

The results of the in vivo study showed that NO-HSA significantly suppressed tumor growth by inducing apoptosis, without adverse changes in serum biochemical parameters in treated mice. In a recent study, Trachootham et al. (2006), using immortalized cell lines and their oncogenic progeny transfected with *H-Ras*^{V12}, demonstrated that cancer cells typically produce more ROS than normal cells. Moreover, the pro-oxidant status of cancer cells increases their susceptibility to treatment with agents that cause oxidative stress, as demonstrated in a study using β-phenylethyl isothiocyanate (Trachootham et al., 2006). In addition, Feng et al. (2007) reported that cyaniding-3-rutinoside selectively induces accumulation of peroxides in HL-60 human leukemic cells, but not in normal peripheral blood mononuclear cells (Feng et al., 2007). Schumacker (2006) has proposed that ROS toxicity induced by certain chemotherapeutic agents may be an effective means of selectively eradicating malignant cells. In the present study, we presumed that although NO reacts with superoxide anion to form peroxynitrite (a potent oxidant and nitrating agent), these highly reactive oxidant species are probably produced at higher

levels in C26 cells compared with normal cells. Therefore, NO-HSA may show selective cytotoxicity for tumor cells and not affect normal cells. These findings strongly suggest that NO-HSA is a promising therapeutic anticancer agent, given the unusual redox conditions typical of malignant cells.

Antiapoptotic effects of NO have been observed in a variety of cells, including T cells, hepatocytes, endothelial cells, neurons, ovarian follicle cells, eosinophils, thymocytes, and embryonic kidney cells (Liu and Stamler, 1999). In a recent study using U937 human promonocytic cells, NO-R410C (a genetic variant of HSA) had antiapoptotic activity (Ishima et al., 2007). Whether NO ultimately inhibits or promotes apoptosis probably depends on the cell, the signal, the source, the molecule, the amount, and the presence or absence of coreactants. For example, the amount of NO bound to the carrier molecule seems to account for the discrepant results between previous investigations and the present study. The NO content of NO-R410C (in the previous study) and NO-HSA (in this study) were 1.3 and 6.6 mol NO/mol HSA, respectively, and the *S*-nitroso moiety concentrations in vitro were 26 to 130 and 165 to 660 μM, respectively. Mohr et al. (1997) reported that 10 to 100 μM GSNO inhibits the activation of caspase-3 induced by actinomycin D in U937 cells. In contrast, apoptosis (characterized by DNA fragmentation and morphological changes) was observed in U937 cells treated with GSNO at concentrations in excess of 250 μM (Messmer et al., 1996). Based on the results of the present study and those of previously published investigations, the critical NO threshold concentration between promotion and inhibition of apoptosis seems to be 100 to 200 μM.

Matsumura et al. (1987) examined the accumulation of differently sized proteins within tumor tissues of tumor-bearing mice. Macromolecules containing HSA tended to accumulate in tumor tissues, apparently due to hypervascularization and enhanced vascular permeability (even to macromolecules) of the tumors, with little export of macromolecules from the tumor tissue via blood or lymphatic vessels (Matsumura et al., 1987). Therefore, NO-HSA may be a useful agent for targeting chemotherapeutics to tumor tissue. However, the short half-life of NO has been one of the greatest obstacles to therapeutic application of NO donors. Consequently, the pharmacokinetic properties of NO-HSA in mice were measured to determine the biological fate of NO. The apparent half-life of *S*-nitroso moieties in NO-HSA was estimated to be 18.9 min (data not shown), which is similar to that of NO-R410C, but much longer than that of the low-molecular-weight NO donor GSNO (4.2 min) (Ishima et al., 2007). In the present study, the difference in NO half-life between NO-HSA and GSNO seemed to be due to reduced renal excretion of HSA compared with glutathione due to its larger molecular size, suggesting that HSA may be a useful NO carrier in vivo.

In summary, NO-HSA was synthesized by inducing *S*-nitrosothiol linkages using iminothiolane as a spacer. NO-HSA generated ROS in C26 cells, and it induced intrinsic apoptotic events, such as depolarization of mitochondrial membrane potentials, activation of caspase-3, and induction of DNA fragmentation. Moreover, NO-HSA inhibited proliferation of tumor cells in vitro in a concentration-dependent manner. In the in vivo experiments, NO-HSA also strongly inhibited tumor growth by inducing apoptosis, with no side effects. The results of the present study suggest that NO-HSA has promise as a new generation anticancer agent with few side effects.

References

Azuma H, Ishikawa M, and Sekizaki S (1986) Endothelium-dependent inhibition of platelet aggregation. *Br J Pharmacol* **88:**411–415.

Beckman JS and Crow JP (1993) Pathological implication of nitric oxide, superoxide and peroxnitrite formation. *Biochem Soc Trans* **21:**330–334.

Brune B, Sandau K, and Knethen AV (1998) Apoptotic cell death and nitric oxide: activating and antagonistic transducing pathways. *Biochemistry (Mosc)* **63:**817–825.

Chen RF (1967) Removal of fatty acids from serum albumin by charcoal Treatment. *J Biol Chem* **242:**173–181.

Ewing JF, Young DV, Janero DR, Garvey DS, and Grinnell TA (1997) Nitrosylated bovine serum albumin derivatives as pharmacologically active nitric oxide congeners. *J Pharmacol Exp Ther* **283:**947–954.

Fabbri F, Brigliadori G, Ulivi P, Tesei A, Vannini I, Rosetti M, Bravaccini S, Amadori D, Bolla M, and Zoli W (2005) Pro-apoptotic effect of a nitric oxide-donating NSAID, NCX4040, on bladder carcinoma cells. *Apoptosis* **10:**1095–1103.

Feng R, Ni HM, Wang SY, Tourkova IL, Shulin MR, Harada H, and Yin XM (2007) Cyanidin-3-rutinoside, a natural polyphenol antioxidant, selectively kills leukemic cells by induction of oxidative stress. *J Biol Chem* **282:**13468–13476.

Gao J, Liu X, and Rigas B (2005) Nitric oxide-donating aspirin induces apoptosis in human colon cancer cells through induction of oxidative stress. *Proc Natl Acad Sci U S A* **102:**17207–17212.

Garthwaite J (1991) Glutamate, nitric oxide and cell-cell signaling in the nervous system. *Trends Neurosci* **14:**60–67.

Gavrieli Y, Sherman Y, and Ben-Sasson SA (1992) Identification of programmed cell death in Situ via specific labeling of nuclear DNA fragmentation. *J Cell Biol* **119:**493–501.

Hibbs JB Jr, Taintor RR, Vavrin Z, and Rachlin EM (1988) Nitric oxide: a cytotoxic activated macrophage effector molecule. *Biochem Biophys Res Commun* **157:**87–94.

Ignarro LJ (1989) Endothelium-derived nitric oxide–pharmacology and relationship to the actions of organic nitrate esters. *Pharm Res* **6:**651–659.

Ishima Y, Sawa T, Kragh-Hansen U, Miyamoto Y, Matsushita S, Akaike T, and Otagiri M (2007) *S*-Nitrosylation of human variant albumin Liprizzi (R410C) confers potent antibacterial and cytoprotective properties. *J Pharmacol Exp Ther* **320:**969–977.

Ishiyama M, Tominaga H, Shiga M, Sasamoto K, Ohkura Y, and Ueno K (1996) A combined assay of cell viability and in vitro cytotoxicity with a highly water-soluble tetrazolium salt, neutral red and crystal violet. *Biol Pharm Bull* **19:**1518–1520.

Kashfi K, Ryann Y, Qiao LL, Williams JL, Chen J, Soldato PD, Traganos FT, and Rigas B (2002) Nitric oxide-donating nonsteroidal anti-inflammatory drugs inhibit the growth of various cultured human cancer cells: evidence of a tissue type-independent effect. *J Pharmacol Exp Ther* **303:**1273–1282.

Kaufmann SH and Gores GJ (2000) Apoptosis in cancer: cause and cure. *Bioessays* **22:**1007–1017.

Kiziltepe T, Hideshima T, Ishitsuka K, Ocio EM, Raje N, Catley L, Li CQ, Trudel LJ, Yasi H, Vallet S, et al. (2007) JS-K, a GST-activated nitric oxide generator, induces DNA double-strand breaks, activates DNA damage response pathways, and induces apoptosis in vitro and in vivo in human multiple myeloma cells. *Blood* **110:**709–718.

Kondo Y, Kanzawa T, Sawaya R, and Kondo S (2005) The role of autophagy in cancer development and response to therapy. *Nat Rev Cancer* **5:**726–734.

Laval F and Wink DA (1994) Inhibition by nitric oxide of the repair protein, O6-methyl-gluanine-DNA-methyltransferase. *Carcinogenesis* **15:**443–447.

Liu L and Stamler JS (1999) NO: an inhibitor of cell death. *Cell Death Differ* **6:**937–942.

Marks DS, Vita JA, Folts JD, Keaney JF Jr, Welch GN, and Loscalzo J (1995). Inhibition of neointimal proliferation intimal proliferation in rabbits after vascular injury by a single treatment with a protein adduct of nitric oxide. *J Clin Investig* **96:**2630–2638.

Marletta MA, Yoon PS, Iyengar R, Leaf CD, and Wishnok JS (1988) Macrophage oxidation of L-arginine to nitrite and nitrate–nitric oxide is an intermediate. *Biochemistry* **27:**8706–8711.

Matsumura Y, Oda T, and Maeda H (1987) General mechanism of intratumor accumulation of macromolecules: advantage of macromolecular therapeutics. *Gan To Kagaku Ryoho* **14:**821–829.

Matsushita S, Ishima Y, Chuang VT, Watanabe H, Tanase S, Maruyama T, and Otagiri M (2004) Functional analysis of recombinant human serum albumin domains for pharmaceutical applications. *Pharm Res* **10:**1924–1932.

Messmer UK, Reimer DM, and Brune B (1996) Nitric oxide-induced apoptosis: p53-dependent and p53-indeoendent signaling pathways. *Biochem J* **319:**299–305.

Meng XW, Lee SH, and Kaufmann SH (2006) Apoptosis in the treatment of cancer: a promise kept? *Curr Opin Cell Biol* **18:**668–676.

Mohr S, Zech B, Lapetina EG, and Brune B (1997) Inhibition of caspase-3 by S-nitrosation and oxidation caused by Nitric oxide. *Biochem Biophys Res Commun* **238:**387–391.

Moncada S and Higgs A (1993) The L-arginine-nitric oxide pathway. *N Engl J Med* **329:**2002–2012.

Moncada S, Palmar RMJ, and Gryglewski RJ (1986) Mechanism of action of some inhibitors of endothelium-derived relaxing factor. *Proc Natl Acad Sci U S A* **83:**9164–9168.

Okada H and Mak TW (2004) Pathways of apoptotic and non-apoptotic death in tumor cells. *Nat Rev Cancer* **4:**592–603.

Peters T Jr (1985) Serum albumin. *Adv Protein Chem* **37:**161–245.

Ramachandran N, Root P, Jiang XM, Hogg OJ, and Mutus B (2001) Mechanism of

transfer of NO from extracellular S nitrosothiols into the cytosol by cell-surface protein disulfide isomerase. *Proc Natl Acad Sci U S A* **98:**9539–9544.
Schumacker PT (2006) Reactive oxygen species in cancer cells: live by sword, die by the sword. *Cancer Cell* **10:**175–176.
Semsroth S, Fellner B, Trescher K, Bernecker OY, Kalinowski L, Gasser H, Hallstrom S, Malinski T, and Podesser BK (2005) S-Nitroso human serum albumin attenuates ischemia/reperfusion injury after cardioplegic arrest in isolated rabbit hearts. *J Heart Lung Transplant* **24:**2226–2234.
Shimizu K, Asai T, Fuse C, Sadzuka Y, Sonobe T, Ogino K, Taki T, Tanaka T, and Oku N (2005) Applicability of anti-neovascular therapy to drug-resistant tumor: suppression of drug-resistant P388 tumor growth with neovessel-targeted liposomal adriamycin. *Int J Pharm* **296:**133–141.
Simon DI, Mullins ME, Jia L, Gaston B, Singel DJ, and Stamler JS (1996) Polynitrosylated proteins: characterization, bioactivity, and functional consequences. *Proc Natl Acad Sci U S A* **93:**4736–4741.
Stamler JS, Jaraki O, Osborne J, Simon DI, Keaney J, Vita J, Singel D, Valeri CR, and Loscalzo J (1992) Nitric oxide circulates in mammalian plasma primarily as an S-nitroso adduct of serum albumin. *Proc Natl Acad Sci U S A* **89:**7674–7677.
Trachootham D, Zhou Y, Zhang H, Demizu Y, Chen Z, Pelicano H, Chiao PJ, Achanta G, Arlinghaus RB, Liu J, et al. (2006) Selective killing of oncogenically transformed cells through a ROS-mediated mechanism by β-phenylethyl isothiocyanate. *Cancer Cell* **10:**241–252.
Williams JL, Borgo S, Hasan I, CastilloE, Traganos F, and Rigas B (2001) Nitric oxide-releasing nonsteroidal anti-inflammatory drugs (NSAIDs) alter the kinetics of human colon cancer cell lines more effectively than traditional NSAIDs: implication for colon cancer chemoprevention. *Cancer Res* **61:**3285–3289.
Wong PS and Fukuto JM (1999) Reaction of organic nitrate esters and S-nitrosothiols with reduced flavins: a possible mechanism of bioactivation. *Drug Metab Dispos* **27:**502–509.

Address correspondence to: Dr. Masaki Otagiri, Department of Biopharmaceutics, Graduate school of Pharmaceutical Sciences, Kumamoto University, 5-1 Oe-honmachi, Kumamoto 862-0973, Japan. E-mail: otagirim@gpo.kumamoto-u.ac.jp

JPET PHARMACOLOGY AND EXPERIMENTAL THERAPEUTICS aspet

✕ Author's Choice

THE JOURNAL OF BIOLOGICAL CHEMISTRY VOL. 283, NO. 50, pp. 34966–34975, December 12, 2008

S-Nitrosylated Human Serum Albumin-mediated Cytoprotective Activity Is Enhanced by Fatty Acid Binding*

Received for publication, September 10, 2008, and in revised form, October 20, 2008 Published, JBC Papers in Press, October 20, 2008, DOI 10.1074/jbc.M807009200

Yu Ishima[‡], Takaaki Akaike[§], Ulrich Kragh-Hansen[¶], Shuichi Hiroyama[‡], Tomohiro Sawa[§], Ayaka Suenaga[‡], Toru Maruyama[‡], Toshiya Kai[‡‖], and Masaki Otagiri[‡1]

From the [‡]Department of Biopharmaceutics, Graduate School of Pharmaceutical Sciences, Kumamoto University, 5-1 Oe-honmachi, Kumamoto 862-0973, Japan, the [§]Department of Microbiology, Graduate School of Medical Sciences, Kumamoto University, 1-1-1 Honjo, Kumamoto 860-8556, Japan, the [¶]Department of Medical Biochemistry, University of Aarhus, DK-8000 Aarhus C, Denmark, and the [‖]Pharmaceutical Research Center, Nipro Corporation, Shiga, Japan

Binding of oleate to *S*-nitrosylated human serum albumin (SNO-HSA) enhances its cytoprotective effect on liver cells in a rat ischemia/reperfusion model. It enhances the antiapoptotic effect of SNO-HSA on HepG2 cells exposed to anti-Fas antibody. To identify some of the reasons for the increased cytoprotective effects, additional experiments were performed with glutathione and HepG2 cells. As indicated by 5,5′-dithiobis-2-nitrobenzoic acid binding, the addition of oleate increased the accessibility of the single thiol group of albumin. Binding of increasing amounts of oleate resulted in increasing and more rapid *S*-transnitrosation of glutathione. Likewise, binding of oleate, or of a mixture of endogenous fatty acids, improved *S*-denitrosation of SNO-HSA by HepG2 cells. Oleate also enhanced *S*-transnitrosation by HepG2 cells, as detected by intracellular fluorescence of diaminofluorescein-FM. All of the *S*-transnitrosation caused by oleate binding was blocked by filipin III. Oleate also increased, in a dose-dependent manner, the binding of SNO-HSA labeled with fluorescein isothiocyanate to the surface of the hepatocytes. A model in two parts was worked out for *S*-transnitrosation, which does not involve low molecular weight thiols. Fatty acid binding facilitates *S*-denitrosation of SNO-HSA, increases its binding to HepG2 cells and greatly increases *S*-transnitrosation by hepatocytes in a way that is sensitive to filipin III. A small nitric oxide transfer takes place in a slow system, which is unaffected by fatty acid binding to SNO-HSA and not influenced by filipin III. Thus, fatty acids could be a novel type of mediator for *S*-transnitrosation.

S-Nitrosothiols may serve as a reservoir of NO in biological systems, and they represent a class of NO donor with many potential biological and clinical uses. In this respect, Cys-34 of human serum albumin (HSA)[2] is important, because it represents the largest fraction of free thiols in circulation (1). In accordance with this proposal, *S*-nitrosylated HSA (SNO-HSA) has been reported to improve systolic and diastolic function, as well as myocardial perfusion and oxygen metabolism, in pigs during reperfusion after severe myocardial ischemia (2, 3) and to reduce ischemia/reperfusion injury in rabbit skeletal muscle (4) and rat liver (5). Among its other beneficial effects, SNO-HSA inhibits the activation of circulating platelets (6), suppresses apoptosis of human promonocytic cells (5), and exhibits antibacterial activity *in vitro* (5).

HSA is a multifunctional protein synthesized and secreted by liver cells. It is a single, non-glycosylated polypeptide that organizes to form a heart-shaped protein with ~67% α-helix but no β-sheet (1). All but one (Cys-34) of the 35 cysteine residues are involved in the formation of stabilizing disulfide bonds. In circulation, approximately half of HSA contains Cys-34 as a free sulfhydryl, whereas the remainder is oxidized or ligand-bound. In addition to forming *S*-nitrosothiols, HSA can interact reversibly with a large number of endogenous and exogenous ligands (1, 7, 8). Thus, one of the important *in vivo* functions of albumin is to transport fatty acids, and usually the protein carries different fatty acid anions, up to a total amount of 1–2 molar equivalents. However, this value can rise to about 4 after maximal exercise or other adrenergic stimulation (1).

In the present work, the effect of oleate (OA) on *S*-transnitrosation from SNO-HSA was studied. OA was used as a representative for the endogenous fatty acids, because quantitatively it is the most important fatty acid in human depot fat, and because it is a major contributor to the albumin-bound fatty acids. First, it was observed that co-binding of OA improved SNO-HSA-mediated cytoprotection against ischemia/reperfusion liver injury in rats and improved its antiapoptotic effect on human hepatocellular carcinoma (HepG2) cells exposed to anti-Fas antibody. In an attempt to explain these effects, *S*-transnitrosation was then investigated in simpler systems, namely from SNO-HSA to glutathione (GSH) and to HepG2 cells. The effect of a mixture of endogenous fatty acids on the latter *S*-transnitrosation was also studied. The influence of OA binding on NO transfer to the HepG2 cells and on the interaction

* This work was supported in part by grants-in-aid from the Japan Society for the Promotion of Science (JSPS), a grant-in-aid from the Ministry of Education, Culture, Sports, Science, and Technology (18390051), Japan, and by Fonden af 1870. The costs of publication of this article were defrayed in part by the payment of page charges. This article must therefore be hereby marked "*advertisement*" in accordance with 18 U.S.C. Section 1734 solely to indicate this fact.

✕ *Author's Choice*—Final version full access.

[1] To whom correspondence should be addressed: 5-1 Oe-honmachi, Kumamoto 862-0973, Japan. Tel.: 81-96-371-4150; Fax: 81-96-362-7690; E-mail: otagirim@gpo.kumamoto-u.ac.jp.

[2] The abbreviations used are: HSA, human serum albumin; SNO-HSA, *S*-nitrosylated HSA; GS-NO, *S*-nitrosylated GSH; OA, oleic acid/oleate; ALT, alanine aminotransferase; AST, asparatate aminotransferase; DAF-FM DA, diaminofluorescein-FM diacetate; FITC, fluorescein isothiocyanate; DTT, 1,4-dithiothreitol; DTNB, 5,5′-dithiobis-2-nitrobenzoic acid; DTPA, diethylenetriaminepentaacetic acid; IAN, isoamyl nitrite; DMEM, Dulbecco's modified Eagle's medium.

between SNO-HSA and the hepatocytes was examined. Finally, a model for the OA-induced improvement of NO transfer to HepG2 cells is proposed.

EXPERIMENTAL PROCEDURES

Materials—Non-defatted HSA (96% pure) was donated by the Chemo-Sera-Therapeutic Research Institute (Kumamoto, Japan), and it was defatted by treatment with charcoal as described by Chen (9). Sephadex G-25 (ϕ 1.6 × 2.5 cm) and Blue Sepharose CL-6B (ϕ 2.5 × 20 cm) were from GE Healthcare (Tokyo, Japan). OA, caprylate, stearate, GSH, 1,4-dithiothreitol (DTT), and filipin III were purchased from Sigma-Aldrich. Isoamyl nitrite (IAN) was purchased from Wako Chemicals (Osaka, Japan). Sulfanilamide, naphthylethylenediamine-hydrochloride, $HgCl_2$, and $NaNO_2$ were obtained from Nakalai Tesque (Kyoto, Japan). Diethylenetriaminepentaacetic acid (DTPA), 5,5′-dithiobis-2-nitrobenzoic acid (DTNB), and fluorescein isothiocyanate (FITC) were bought from Dojindo Laboratories (Kumamoto, Japan). Dulbecco's modified Eagle's medium (DMEM) was from Invitrogen (Rockville, MD), and diaminofluorescein-FM diacetate (DAF-FM DA) was from Daiichi Pure Chemicals (Tokyo, Japan). $^{111}InCl_3$ (74 MBq/ml in 0.02 N HCl) was a gift from Nihon Medi-Physics Co., Ltd. (Hyogo, Japan). The other chemicals were of the best grades commercially available, and all solutions were made in deionized and distilled water.

S-Nitrosylation of HSA—*S*-Nitrosylated protein was prepared with protection against light and according to previously reported methods (10, 11). First, HSA (300 μM) was incubated with DTT (molar ratio, protein:DTT = 1:10) for 5 min at 37 °C. After incubation, DTT was immediately removed by Sephadex G-25 gel filtration and eluted with 0.1 M potassium phosphate buffer (pH 7.4) containing 0.5 mM DTPA. Samples of 0.1 mM DTT-treated protein (0.8 mol sulfhydryl groups/mol protein) were then incubated with IAN (molar ratio, protein:IAN = 1:10) in 0.1 M potassium phosphate buffer (pH 7.4) containing 0.5 mM DTPA for 60 min at 37 °C. The amount of the *S*-nitroso moiety of SNO-HSA was quantified by HPLC coupled with a flow-reactor system, as previously reported (10). The HPLC column was a gel filtration column for *S*-nitrosylated proteins (ϕ 8 × 300 mm), Diol-120, YMC, Kyoto, Japan. Briefly, the eluate from the HPLC column was mixed with a $HgCl_2$ solution to decompose *S*-nitrosylated compounds to yield NO_2^- (via NO^+). The NO_2^- generated was then detected after reaction with Griess reagent in the flow-reactor system. Controls performed in the absence of $HgCl_2$ gave no protein-derived absorbency at 540 nm after reaction with the Griess reagent. Therefore, non-covalent association of the nitrite anion with albumin can be excluded. The *S*-nitrosylated product (0.35 ± 0.04 mol SNO-groups/mol protein; mean ± S.E., n = 53) was purified by Sephadex G-25 gel filtration, eluted with 0.1 M potassium phosphate buffer (pH 7.4) containing 0.5 mM DTPA, and concentrated by ultrafiltration (cutoff size of 7500 Da). These samples were stored at −80 °C until use. The protein content of all protein preparations used in this study was determined using the Bradford assay.

Binding of Fatty Acid to HSA—A stock solution of 20 mM OA was made in methanol-H_2O (1:1, v/v). Aliquots of the OA stock solution were added to HSA or SNO-HSA and dissolved in 0.1 M potassium phosphate buffer (pH 7.4) to give OA:HSA molar ratios of 1, 3, or 5; the maximal methanol concentration in the final solutions was 1.25%. Before use, the solutions were held at 37 °C for 30 min. The amount of bound OA was checked using the following approach. The solutions containing albumin and OA were applied to a Sephadex G-25 gel filtration column, the protein-containing fractions were pooled, and both the protein and OA concentrations in the pooled material were determined. The OA concentrations were determined by a colorimetric method using a commercial kit (WAKO NEFA kit) according to the manufacturer's instructions. Three standards (0.5, 1.0, and 1.97 mEq/liter) supplied by the vendor were used to establish a standard curve for determination of the concentration of OA.

Cytoprotective Effect of SNO-HSAs in Vivo—A rat ischemia/reperfusion liver injury model was used to investigate the cytoprotective effect of SNO-HSA, as previously reported (5, 11). Male Wistar rats weighing between 200 and 230 g (Kyudo, Inc., Kumamoto, Japan) were used. The animals were fasted for 9 h before surgery, but were allowed access to water. The rats were anesthetized with ether during the operation. After the abdomen was shaved and disinfected with 70% ethanol, a complete midline incision was made. The portal vein and hepatic artery were exposed and cross-clamped for 30 min with a noncrushing microvascular clip. Saline, as the vehicle control, or HSA or SNO-HSA (0.1 μmol/rat) with or without bound OA was given via the portal vein immediately after reperfusion was initiated. Because the blood volume of a 200-g rat was estimated to be about 10 ml, we expected blood levels of SNO-HSA to reach ~3 μM after administration of 0.1 μmol/rat of SNO-HSA. This concentration of SNO-HSA is a physiologically relevant one, because levels of *S*-nitrosothiols in normal plasma are at the most 7 μM (12). The abdomen was then closed in two layers with 2–0 silk. The rats were kept under warming lamps until they awakened and became active.

Because blood loss caused by frequent blood sampling could affect liver function, the animals were euthanized by taking whole circulating blood via the abdominal aorta under anesthesia at various time points after reperfusion was initiated. Plasma alanine aminotransferase (ALT) and aspartate aminotransferase (AST) activities were measured by using a sequential multiple AutoAnalyzer system from Wako Chemicals, with activities expressed in international units per liter. All the animal experiments were carried out according to the guidelines of the Laboratory Protocol of Animal Handling, Graduate School of Medical Sciences, Kumamoto University.

Antiapoptotic Effect of SNO-HSA in Vitro—HepG2 cells (2×10^5 cells/well) were cultured in 96-well plates (16-mm diameter; Falcon, Lincoln Park, NJ) with DMEM supplemented with 10% fetal bovine serum (Invitrogen). The cells were maintained in a humidified incubator (95% air, 5% CO_2) for 12 h at pH 7.4 and 37 °C. Afterwards, they were treated with different concentrations of HSA or SNO-HSA, with and without bound OA, for 6 h in the dark. The cells were then washed three times with 10 mM phosphate-buffered saline (pH 7.4) to remove the remaining SNO-HSA. After washing, the cells were reacted with 400 ng/ml anti-Fas antibody (Medical and Biological Laboratories,

Nagoya, Japan). After 15 h of incubation, the cultures were treated with 0.05% trypsin, and the cells were transferred to Eppendorf tubes (1.5 ml). The number of apoptotic cells was determined by an annexin V-FITC binding assay kit from BD Biosciences (Tokyo, Japan). The fluorescence of annexin V-FITC and propidium iodide were measured by a FACSCalibur flow cytometer.

Pharmacokinetic Experiments—SNO-HSA, with and without OA, was labeled with ^{111}In, using DTPA anhydride as a bifunctional chelating agent (13, 14). Labeled proteins were injected via the tail vein into male ddY mice (weighing 25–27 g) at a dose of 0.1 mg/kg. At appropriate times after injection, blood was collected from the vena cava with the mouse under ether anesthesia. Heparin sulfate was used as an anticoagulant, and plasma was obtained from the blood by centrifugation. Liver, kidney, and spleen samples were obtained, rinsed with saline, and weighed. The radioactivity in each sample was counted using a well-type NaI scintillation counter ARC-2000 (Aloka, Tokyo, Japan). ^{111}In radioactivity concentrations in plasma were normalized as a percentage of the dose per milliliter and analyzed using the nonlinear least-squares program MULTI (15). Organ distribution profiles were evaluated by relating the radioactivity per gram of tissue to the total amount of injected radioactivity.

Accessibility of Cys-34—We determined the accessibility of Cys-34 in reduced HSA with Ellman's reagent, DTNB (16, 17). HSA (300 μM), with and without OA, and DTNB (5 mM) were mixed in 0.1 M potassium phosphate buffer (pH 7.0) at 20 °C, and the absorbance at 450 nm was registered as a function of time.

S-Denitrosylation of SNO-HSA by GSH and by HepG2 Cells—Solutions with both 100 μM SNO-HSA and 100 μM GSH were made in 10 mM phosphate-buffered saline, pH 7.4. Then 0-, 7.5-, 15-, and 30-min samples were taken, mixed with 1/10 volume of 5 mM DTPA (pH 7.4) and placed at −80 °C. The concentrations of the remaining SNO-HSA and the *S*-nitrosylated GSH (GS-NO) formed were then determined separately by the HPLC flow reactor system.

HepG2 cells (5×10^5 cells/well) were cultured and incubated with DMEM and fetal bovine serum, as described above. After incubation, the culture medium was removed, and the hepatocytes were washed three times with 10 mM phosphate-buffered saline, pH 7.4. Cells were further incubated at 37 °C in the CO_2 incubator with 200 μl of 10 mM phosphate-buffered saline, pH 7.4 and 100 μM SNO-HSA with different molar ratios of bound OA. Samples were taken after incubation for 0, 15, 30, or 60 min, mixed with 1/10 volume of 5 mM DTPA, pH 7.4 and centrifuged at 10,000 × *g* for 10 min at 4 °C. These supernatants were stored at −80 °C until applied to the HPLC flow reactor system.

HSA Obtained from Hemodialysis Patients—It is known that fatty acids bound to HSA rise by dialysis. The content of fatty acids bound to HSA isolated from hemodialysis patients before and after dialysis was analyzed, and the influence on *S*-denitrosation of fatty acid binding was examined. HSA samples were obtained from hemodialysis patients before (HSA-hd (−)) and after dialysis (HSA-hd (+)) according to a previously reported protocol (18). In brief, albumin concentrations in blood plasma were measured using a diagnostic kit (Biotech Reagent) based on the bromcresol green method. Non-esterified fatty acids were measured using a diagnostic kit from Wako Chemicals (Osaka, Japan). To isolate HSA from patient sera, polyethylene glycol fractionation of blood plasma was followed by chromatography on a Blue Sepharose CL-6B column. After isolation, the samples were dialyzed against deionized water for 48 h at 4 °C, followed by lyophilization. The purity of the HSA-hd samples was at least 95%, and the percentage of dimers did not exceed 7%, as evidenced by SDS-PAGE and native PAGE, respectively. The protocol used in this study was approved by the Institutional Review Board, and informed consent was obtained from all subjects.

Preparation of S-Nitrosylated HSA-hd—HSA-hd (−) or HSA-hd (+) was *S*-nitrosylated using IAN, as described above. The content of SNO groups in SNO-HSA-hd was determined to be (0.35 ± 0.04 for HSA-hd (−) or 0.39 ± 0.06 for HSA-hd (+) mol SNO-groups/mol protein; mean ± S.E., $n = 7$).

S-Denitrosylation of Hemodialysis Patient SNO-HSA by HepG2 Cells: Effects of HSA-bound Fatty Acids—One-hundred micromolar of SNO-HSA-hd (−) and SNO-HSA-hd (+) dissolved in phosphate-buffered saline was incubated with HepG2 cells (5×10^5 cells/well). After 15-, 30-, and 60-min incubation, culture supernatant was collected, and the remaining SNO content was measured and compared with control SNO-HSA samples before incubation.

NO Uptake by HepG2 Cells—HepG2 cells (5×10^5 cells/well) were cultured and incubated with DMEM and fetal bovine serum, as described above. After incubation, the culture medium was removed, and the hepatocytes were washed three times with 10 mM phosphate-buffered saline, pH 7.4. After adding phosphate-buffered saline containing 5 μM DAF-FM DA, the cells were incubated for 1 h in the dark at 37 °C. The cells were again washed three times with phosphate-buffered saline, and further incubated at 37 °C with 100 μM HSA or SNO-HSA with different molar ratios of bound OA. Upon cellular uptake, ester groups in DAF-FM DA are cleaved by esterases, resulting in the formation of DAF-FM that can react with NO to give fluorescence. The fluorescence was determined with excitation at 385 nm and monitored at 535 nm using a monochromator (TECAN SPECTRA FLUOR). In some experiments, 50 μM filipin III (caveolae formation inhibitor) dissolved in phosphate-buffered saline was added after 30 min of DAF-FM DA exposure (19).

Binding of FITC-HSA to HepG2 Cells—The binding of HSA to HepG2 cells, with or without *S*-nitrosylation and its modulation by fatty acid binding, was analyzed by means of fluorescent microscopy with HSA labeled with FITC. FITC-HSA was prepared according to a previous report (20). In short, HSA (60 μM) was incubated with FITC (2 mM) for 3 h at 25 °C in 0.1 M potassium phosphate buffer (pH 7.4). After incubation, FITC-HSA was isolated from unreacted FITC using a Sephadex G-25 gel with the phosphate buffer, and stored at −80 °C until use. To prepare FITC-SNO-HSA, HSA was first *S*-nitrosylated as described above, followed by FITC labeling. After purification of FITC-SNO-HSA, the SNO content was determined to be (0.33 ± 0.03 mol SNO-groups/mol protein; mean ± S.E., $n = 3$),

suggesting that FITC labeling did not affect the SNO content to a significant extent.

For the binding assay, HepG2 cells (5×10^5 cells/well) were preincubated with serum-free DMEM for 2 h at 37 °C. In some experiments, cells were further treated with 50 μM filipin III for 30 min, which inhibits caveolae formation. Cells were then maintained at 4 °C to block the uptake of macromolecules through energy-dependent mechanisms, including endocytosis. FITC-SNO-HSA with varying OA content (0, 3, 5 OA/HSA) was dissolved in 10 mM phosphate-buffered saline, pH 7.4 and added to the culture wells to give a final concentration of 50 μg/ml. After 10 min, the cells were washed twice with phosphate-buffered saline to remove unbound FITC-SNO-HSA and fixed with 4% paraformaldehyde in phosphate-buffered saline at 25 °C for 30 min. After washing twice in MilliQ water, these cells were analyzed using a fluorescence microscope (Biozero-8000, Keyence, Osaka, Japan) with the combination of excitation at 385 nm and emission at 535 nm. Fluorescent intensity was quantified using an NIH Image. Similar experiments were conducted using FITC-HSA without *S*-nitrosylation.

Statistical Analysis—The statistical significance of the collected data were evaluated using analysis of variance, followed by the Newman-Keuls method for more than 2 means. Data are expressed as means ± S.E. Differences between groups were evaluated using a Student's *t* test. $p < 0.05$ was regarded as statistically significant.

RESULTS

Effect of OA Binding on SNO-HSA-mediated Cytoprotection against Ischemia/Reperfusion Liver Injury in Rats—An ischemia/reperfusion liver injury model (5) was used to examine the *in vivo* effect of OA binding on SNO-HSA-mediated cytoprotection. Because previous studies with SNO-HSA showed that a quantity of 0.1 μmol/rat had the greatest protective effect (5), the same quantity was used in this study. To evaluate liver injury, the extracellular release of the liver enzymes AST and ALT was measured via plasma enzyme values. Injecting HSA, OA, or HSA-OA into the portal vein immediately after reperfusion was initiated did not affect the plasma concentrations of AST and ALT (data not shown). However, administration of SNO-HSA diminished, to a significant extent, the enzyme concentrations measured after 60 and 120 min (Fig. 1). The protection of the liver cells by SNO-HSA was more pronounced if the protein also carried OA; the additive effect was most evident after 120 min of reperfusion. The effect of OA on SNO-HSA-mediated cytoprotection appears to depend on OA content, *e.g.* AST release was reduced significantly more by treatment with SNO-HSA-OA5 than with SNO-HSA-OA3 120 min after reperfusion (Fig. 1*A*). Even at 12 h after reperfusion, the levels of AST and ALT remained significantly lower in SNO-HSA-OA-treated animals than in control animals, although the differences were not so pronounced as those observed at 120 min after reperfusion (data not shown). We also examined the effect of other fatty acid on cytoprotective effect for SNO-HSA. In the ischemia/reperfusion injury model, we found that caprylate (C8:0), a short-chain and saturated fatty acid, potentiated the cytoprotective effect of SNO-HSA. The potentiation effect of caprylate was slightly weaker than that of OA. AST levels at 120 min after reperfusion were 3256 ± 55, 2586 ± 105, 2202 ± 253 for treatment with SNO-HSA, SNO-HSA-caprylate (HSA: caprylate = 1:5), SNO-HSA-OA5, respectively (The values are means ± S.E., $n = 4$).

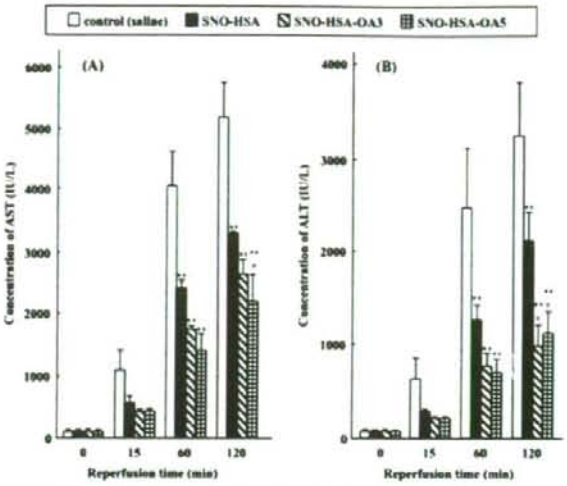

FIGURE 1. **Time profile of changes in serum levels of AST (*A*) and ALT (*B*) after hepatic ischemia/reperfusion in rats.** Ischemia was induced by occluding both the portal vein and hepatic artery for 30 min. After that period of time reperfusion was established. Control (saline), 0.1 μmol of SNO-HSA per rat, or 0.1 μmol of SNO-HSA-OA (OA/HSA = 3 or 5) per rat was administered via the portal vein immediately after initiation of reperfusion. Blood was collected from the portal vein at various time points after reperfusion. ALT and AST activities were measured by using a sequential multiple AutoAnalyzer system. Data are expressed as means ± S.E. ($n = 4$ at each time point). *, $p < 0.05$ and **, $p < 0.01$, compared with control. #, $p < 0.05$, compared with the SNO-HSA-treated group. (OA/HSA = 3 or 5: HSA with 3 or 5 bound OA molecules per protein molecule.)

Effect of OA Binding on SNO-HSA-mediated Cytoprotection of HepG2 Cells Exposed to Anti-Fas Antibody—NO and related species reportedly induce both antiapoptotic and proapoptotic responses in cells, the type of response depending on the concentration of the NO donors and on the type of cell and apoptosis-inducing reagent (5). In the present study, the influence of OA binding on the antiapoptotic effect of SNO-HSA on HepG2 cells treated with anti-Fas antibody was examined. As seen in Fig. 2, the presence of HSA, with or without bound OA, had no effect on the induced apoptosis. OA alone possessed no antiapoptotic activity in our HepG2 cell study (data not shown). By contrast, the addition of SNO-HSA resulted in concentration-dependent protection of the cells. This protection was greatly increased by binding 5 mol of OA per mol of SNO-HSA. Thus, fatty acid binding can also improve the cytoprotective effect of SNO-HSA in an *in vitro* system.

Pharmacokinetic Experiments—The pharmacokinetic characteristics of SNO-HSA with and without bound OA were determined in mice. The results in Fig. 3*A* indicate that OA binding did not affect the elimination of SNO-HSA from the circulation. The plasma half-lives were 269.3 ± 1.7 min, 270.6 ± 1.2 min, and 271.6 ± 5.5 min for SNO-HSA, SNO-HSA-OA3, and SNO-HSA-OA5, respectively. Likewise, the uptake of SNO-HSA by liver, kidney, and spleen was unaffected by OA binding (Fig. 3, *B–D*). These data suggest that binding of

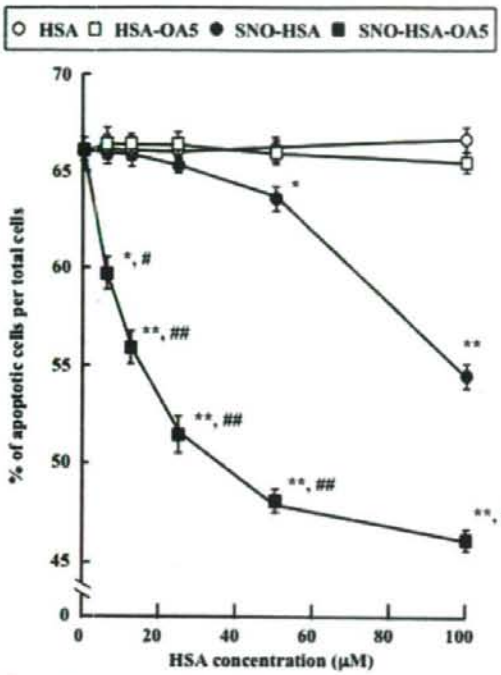

FIGURE 2. **Antiapoptotic effect of albumin without and with 5 mol OA/mol protein.** HepG2 cells (2×10^5 cells/well) were treated with different concentrations (0, 6.25, 12.5, 25, 50, 100 μM) of HSA or SNO-HSA, with and without bound OA, for 6 h at 37 °C in the dark. After incubation, the cells were washed three times with 10 mM phosphate-buffered saline, pH 7.4 to remove the remaining protein. Afterwards, the HepG2 cells were treated with anti-Fas antibody to induce apoptotic cell death. The number of apoptotic cells was determined by means of flow cytometry with annexin V-FITC and propidium iodide. Data are expressed as means ± S.E. ($n = 6$). *, $p < 0.05$ and **, $p < 0.01$, compared with the HSA-treated group. #, $p < 0.05$, ##, $p < 0.01$, compared with the SNO-HSA-treated group.

as much as 5 mol of OA per mol of protein does not modify the pharmacokinetic properties of SNO-HSA.

Accessibility of Cys-34 in HSA-OA—Crystallographic studies have revealed the existence of seven OA binding sites in HSA, and showed that none of these sites involve Cys-34 (21) (Fig. 4*A*). Cys-34 is located in a crevice on the surface of the protein in subdomain IA (1). Therefore, the improvement effect of even the highest OA concentration on the cytoprotection of SNO-HSA must be caused by indirect means. To test this hypothesis, the effect of OA on the readiness of Cys-34 in reduced HSA to bind DTNB was investigated. As seen in Fig. 4*B*, because the amount of DTNB bound after 120 min of incubation was the same without OA and with different concentrations of OA, OA did not mask the thiol in Cys-34. On the contrary, the OA-induced conformational changes enhanced the accessibility of the SH group of Cys-34, because the absorbance at 450 nm increased in a concentration-dependent manner at shorter incubation times. For example, the ratio between the absorbencies after 5 and 120 min of incubation increased from 0.171 ± 0.017 (OA/HSA = 0) to 0.211 ± 0.057 ($p < 0.05$) at OA/HSA = 3 and to 0.821 ± 0.054 ($p < 0.01$) at OA/HSA = 5; the results are given as means ± S.E. ($n = 4$). Non-reducing SDS-PAGE showed that OA binding did not result in dimerization of the protein (data not shown).

S-Denitrosylation of SNO-HSA by GSH and by HepG2 Cells—In Fig. 5*A* it can be seen that OA facilitated *S*-transnitrosation from SNO-HSA to GSH. However, the effect was not dependent on the concentration of OA. The amount of GS-NO formed after 30 min of incubation was higher when OA was bound to SNO-HSA, but the amounts were similar, whether SNO-HSA bound 1, 3, or 5 mol of OA per mol of protein. OA also increased the velocity with which GSH was *S*-nitrosylated. For the sake of comparison, $T_{½}$ values for *S*-transnitrosation were estimated. $T_{½}$ for *S*-nitrosylation of GSH by SNO-HSA was 22 min, whereas $T_{½}$ was only 16 min when *S*-nitrosylation was brought about by SNO-HSA binding 1, 3, or 5 mol OA/mol protein. These findings suggest that only the protein conformational changes caused by binding of the first OA molecule are essential for *S*-transnitrosation to GSH.

The effect of OA on the decay of SNO-HSA was also tested in a biological system using HepG2 cells. From Fig. 5*B*, it is apparent that the decrease in SNO-HSA caused by this cell type was faster and quantitatively more pronounced in the presence of OA, and that the effects increased with OA concentration. Thus, the decrease after 60 min of incubation was significantly greater between 0 and 1, and between 3 and 5 mol OA/mol protein, whereas the increment was smaller when increasing from 1 to 3 mol OA/mol protein. The $T_{½}$ values decreased from 52 min to 24, 22, and 15 min when the amount of OA increased from 0 to 1, 3, and 5 mol/mol protein, respectively. The OA-mediated promotion of SNO-HSA decay can be explained by increased accessibility to the *S*-nitroso moiety of HSA and/or by an intensified interaction between SNO-HSA and cell surface thiols.

S-Denitrosylation of SNO-HSA using HSA Isolated from Hemodialysis Patients—HSA samples obtained from hemodialysis patients were used to study the effect of endogenous fatty acids on *S*-denitrosylation of SNO-HSA. Serum fatty acid concentrations were significantly higher after dialysis among the patients examined (Table 1). Previous studies have shown that the primary fatty acid component in serum from dialysis patients is OA, and that the increased concentration is caused by activation of lipoprotein lipase by administered heparin (22, 23). As shown in Fig. 6, *A* and *B*, the decrease in SNO-HSA caused by HepG2 cells occurred more rapidly for SNO-HSA-hd (+) than SNO-HSA-hd (−). When the $T_{½}$ values of *S*-denitrosylation were plotted against the fatty acid contents in HSA, a good linear fit was obtained (Fig. 6*C*). Taken together, these findings indicate that in addition to OA, endogenous fatty acids can also facilitate the decay of SNO-HSA by HepG2 cells.

NO Uptake of HepG2 Cells—Figs. 5*B* and 6 show that fatty acid binding accelerates the SNO-HSA decomposition by HepG2 cells. To investigate whether this decomposition is accompanied by NO uptake by the cells, we used intracellular DAF-FM fluorescence. From Fig. 7 it is apparent that the intracellular NO concentration increases with incubation time and with increasing OA/SNO-HSA molar ratios. Control experiments performed by incubating HepG2 cells with HSA alone showed no increase in DAF-FM fluorescence (data not shown). To clarify the *S*-transnitrosation properties of other fatty acids,

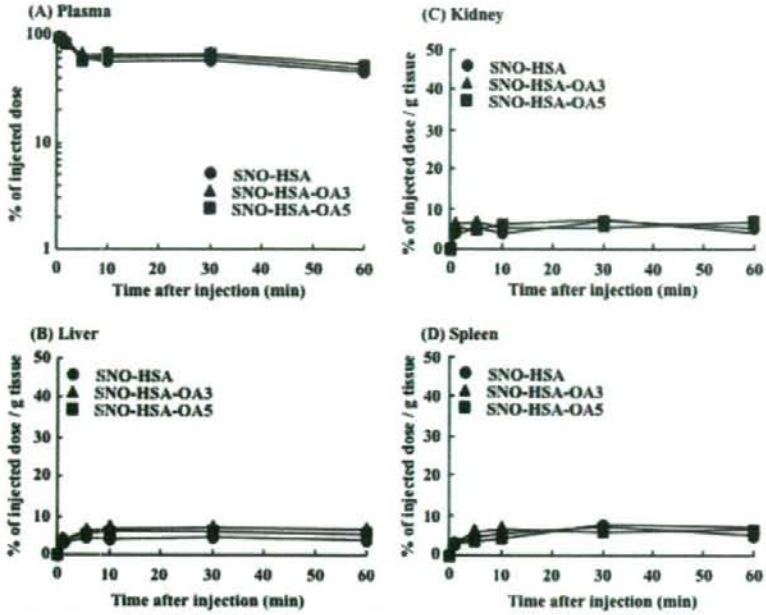

FIGURE 3. **Plasma concentrations of ^{111}In radioactivity (*A*) and tissue accumulation of radioactivity in liver (*B*), kidney (*C*), and spleen (*D*) after i.v. injection of SNO-HSA with different molar ratios of bound OA.** ^{111}In-SNO-HSAs with and without OA were injected via the tail vein into male ddY mice at a dose of 0.1 mg/kg. At different times thereafter, mice were taken for collection of blood from the vena cava with the animal under ether anesthesia; plasma was obtained from the blood by centrifugation. After blood collection, the mice were euthanized, liver, kidney, and spleen samples were obtained, rinsed with saline, and weighed. The radioactivity in each sample was counted using a well-type NaI scintillation counter ARC-2000. Data are expressed as means ± S.E. (n = 3); the *bars* showing S.E. were smaller than the size of the symbols.

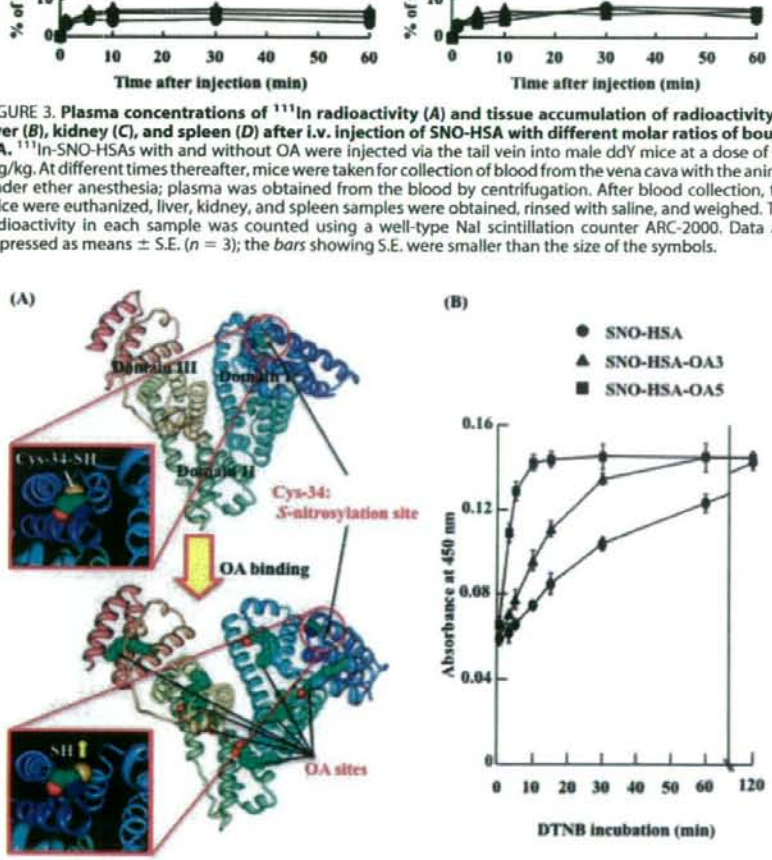

FIGURE 4. **Crystal structure of HSA showing locations of OA binding sites and the *S*-nitrosylated site (Cys-34) (*A*), and the effect of OA binding on the accessibility of Cys-34 (*B*).** *A*, as seen, OA binding results in a more open protein structure. The subdivision of HSA into domains (I-III) is indicated. The structures were simulated on the basis of x-ray crystallographic data for HSA and HSA-OA (PDB ID codes 1bmo and 1gni, respectively) and modified with the use of Rasmol. *B*, SNO-HSA (300 μM), without and with different amounts of bound OA, and DTNB (5 mM) were mixed in 0.1 M potassium phosphate buffer, pH 7.0 at 20 °C, and the absorbance at 450 nm was registered as a function of time. Data are expressed as means ± S.E. (n = 4).

we tested the effect of the saturated fatty acid stearate on NO uptake by HepG2 cells. The results showed that stearate has an effect on the *S*-transnitrosation of SNO-HSA, which is very similar to that of OA (data not shown). From Fig. 7 it can also be seen that the OA-induced increment in the transfer of NO from SNO-HSA into the hepatocytes can be completely blocked by the addition of filipin III.

Binding of SNO-HSA to HepG2 Cells—FITC-fluorescence was used to monitor albumin binding to the cell membrane or membrane components of HepG2 cells. Fig. 8*A* shows a pronounced binding of FITC-SNO-HSA to the hepatocytes. However, 5 equivalents of OA more than doubled albumin binding, to an extent that was significantly higher than that observed upon albumin binding of 3 OA equivalents, which again was significantly higher than that observed in the absence of OA (Fig. 8*E*). Similar results were obtained with albumin that was not *S*-nitrosylated (data not shown). Therefore, albumin binding to HepG2 cells is not affected by *S*-nitrosylation. Finally, the influence of filipin III was investigated. Even though a small decrease in albumin binding was observed (Fig. 8*E*), the decrease was not significant. The present data lead to the proposal that OA binding enhances, in a dose-dependent manner, the interaction between SNO-HSA and HepG2 cells.

DISCUSSION

The *S*-nitrosothiol fraction in plasma is largely composed of SNO-HSA (24). The biological importance of this form of albumin is illustrated by an increasing number of examples of its beneficial effects (2–6). In the present work, its cytoprotective effect on liver cells was used as an example. In addition to forming SNO-HSA, albumin can reversibly bind a large number of endogenous and exogenous ligands (1, 7, 8). Therefore, we sought to investigate whether ligand binding can influence biological activities of

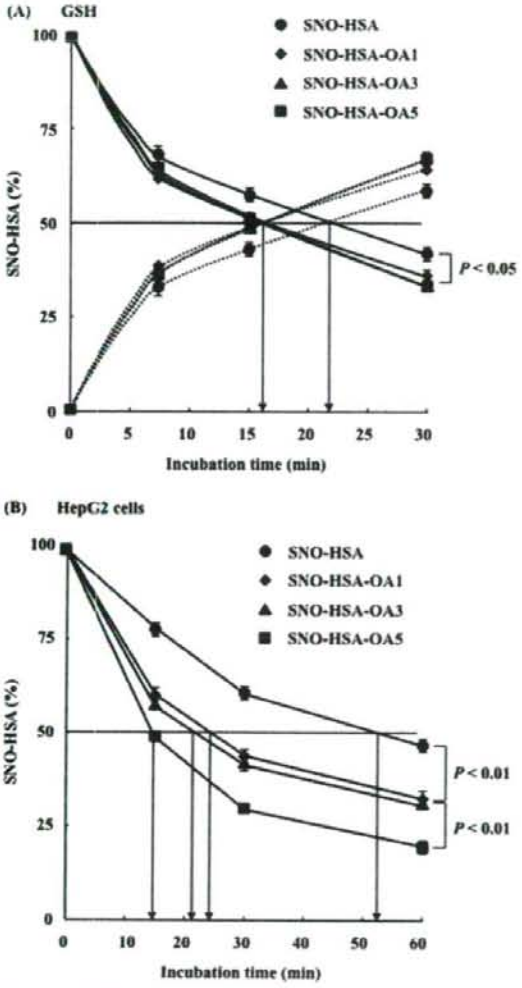

FIGURE 5. **S-Denitrosylation of SNO-HSA by GSH (*A*) and HepG2 cells (*B*).** *A*, SNO-HSA (100 μM), without and with different amounts of bound OA, was incubated with GSH (100 μM) in 10 mM phosphate-buffered saline, pH 7.4 at 37 °C. After 0, 7.5, 15, and 30 min of incubation, samples were taken, and the concentrations of the remaining SNO-HSA (*full curves*) and the GS-NO formed (*dotted curves*) were determined separately by a HPLC flow reactor system. The $T_{1/2}$ values for the decline of SNO-HSAs are indicated by the *arrows*. *B*, SNO-HSA (100 μM), without and with different amounts of bound OA, was incubated with HepG2 cells (5×10^5 cells/well) in 10 mM phosphate-buffered saline, pH 7.4 at 37 °C. After 0, 15, 30, or 60 min of incubation, the concentrations of the remaining SNO-HSA were determined by the HPLC flow reactor system. The $T_{1/2}$ values for the decline of SNO-HSAs are indicated. Data are expressed as means ± S.E. ($n = 3$). *, $p < 0.05$ and **, $p < 0.01$, compared with SNO-HSA without OA binding.

SNO-HSA with particular reference to its cytoprotective effects. As seen in Fig. 1, binding of the important endogenous fatty acid OA increased the cytoprotective effect on liver cells in a dose-dependent manner. The effect may involve multiple mechanisms, including maintenance of tissue blood flow, induction of heme oxygenase-1 (a cytoprotective enzyme), suppression of neutrophil infiltration and reduction of apoptosis (11).

As a first step, we tested whether binding of OA could also increase the cytoprotective effect of SNO-HSA in an *in vitro* system. This was found to be the case, because OA enhanced the antiapoptotic effect of SNO-HSA on HepG2 cells exposed to anti-Fas antibody (Fig. 2). One explanation for the improvement effect of OA binding is an increased accessibility to the *S*-nitrosothiol group of HSA (Fig. 4). From the crystal structure analyses (16, 21, 25), it has been suggested that the reactive SH group of Cys-34 is located in a crevice on the surface of the HSA. Binding of oleate to HSA has been reported to induce conformational changes in the protein, leading to the slight opening of the interface between the two halves of the albumin molecule and a rotation of domain I to open the crevice that contains Cys-34, results in the increase of the accessibility of the Cys-34 SH group (25). The binding of only one mol of OA per mol of SNO-HSA was sufficient to increase *S*-transnitrosation to the relatively small GSH molecule (Fig. 5*A*). By contrast, the decay of SNO-HSA caused by incubation with HepG2 cells increased with the OA concentration up to a SNO-HSA:OA molar ratio of 5 (Fig. 5*B*). Essentially, the same effect was observed with SNO-HSA to which a mixture of endogenous fatty acids was bound (Fig. 6). This finding has biological and clinical implications, because the plasma concentration of non-esterified fatty acids can be increased in a number of situations. In addition to hemodialysis (Table 1), the increase in fatty acids is seen in connection with exercise and other adrenergic stimulation, and in pathological conditions such as the metabolic syndrome and diabetes mellitus.

TABLE 1

Plasma concentrations of HSA and fatty acids in 7 patients before and after hemodialysis

The concentrations of albumin are after dialysis, but they were not significantly affected by dialysis. Results are expressed as means ± S.E. ($n = 3$–4). *p* values for before and after dialysis.

	Sex	Albumin	Number of dialysis	Fatty acids		*p* values
				Before dialysis	After dialysis	
		g/dl		*mM*	*mM*	
No.1	F	2.9 ± 0.2	4	0.070 ± 0.003	0.159 ± 0.003	0.000973
No.2	F	3.9 ± 0.4	12	0.114 ± 0.004	0.614 ± 0.006	0.000624
No.3	F	4.0 ± 0.3	10	0.174 ± 0.005	0.261 ± 0.003	0.000323
No.4	F	3.6 ± 0.3	4	0.182 ± 0.006	0.934 ± 0.007	0.000546
No.5	M	4.1 ± 0.2	3	0.322 ± 0.005	0.718 ± 0.005	0.000478
No.6	M	3.9 ± 0.4	8	0.230 ± 0.005	0.380 ± 0.003	0.000556
No.7	F	4.1 ± 0.3	18	0.130 ± 0.005	0.651 ± 0.003	0.000236

Two additional factors in the improvement effect of OA binding are proposed by the present work. First, the decomposition of SNO-HSA seen in the presence of HepG2 cells is accompanied by a pronounced filipin III-sensitive *S*-transnitrosation of intracellular components (Fig. 7). A basal mechanism, not affected by filipin III addition, results in the slow transfer of small amounts of NO or modifications thereof (*e.g.* NO^+, Fig. 7). The filipin III-sensitive system is faster and quantitatively more important; it is activated by OA. Both systems may involve a membrane protein, and they may operate by transferring NO^+ from one thiol to another. The second factor is an OA-mediated increased interaction between SNO-HSA and the hepatocytes (Fig. 8). As established by the seminal study of Stremmel *et al.*, HSA-fatty acid complexes possess a high affinity to the caveolae (27, 28). Therefore, the structure of caveolae is essential for cellular fatty acid uptake.

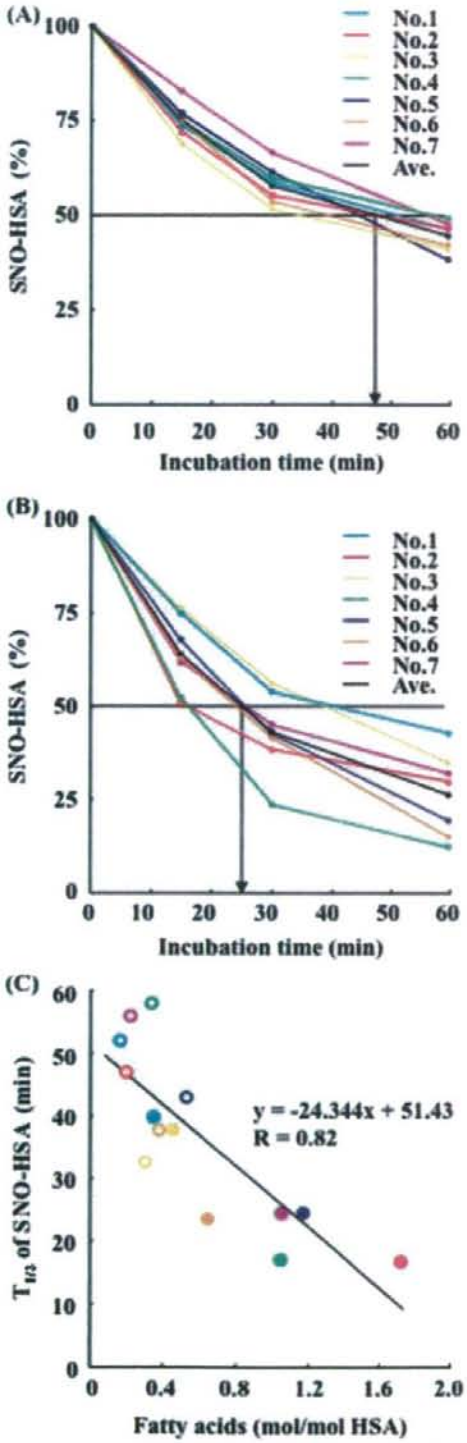

FIGURE 6. **S-Denitrosylation of SNO-HSA made from HSA isolated from hemodialytic patients before (*A*) and after (*B*) dialysis by HepG2 cells.** HSA samples were obtained from hemodialytic patients before and after dialysis. The HSA samples were *S*-nitrosylated using IAN, as described above. HepG2 cells (5×10^5 cells/well) and 100 μM SNO-HSA having different amounts of bound endogenous fatty acids were incubated in 10 mM phosphate-buffered saline, pH 7.4 at 37 °C. After 15, 30, and 60 min of incubation, the concentration of the remaining SNO-HSA was measured by the HPLC flow reactor system. The average $T_{1/2}$ for the *S*-denitrosylation is indicated, *i.e.* 48 min in *A* and 25 min in *B*. Data are expressed as means of four experiments. *C*, relationship between the individual $T_{1/2}$ values and the fatty acid contents of the HSA samples used. Samples are represented by *open circles* (before dialysis) or by *closed circles* (after dialysis); the colors correspond to the hemodialytic patients' number and color in *panel A* and *panel B*.

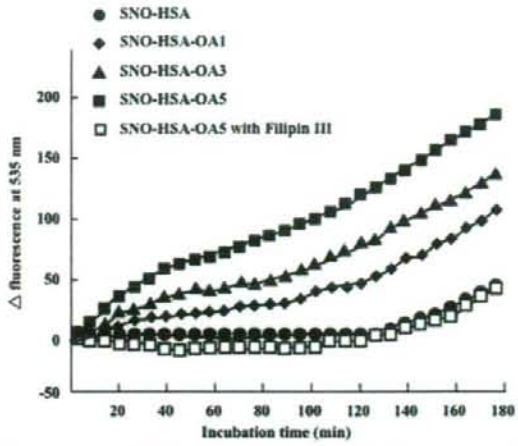

FIGURE 7. **Intracellular NO concentration of HepG2 cells exposed to SNO-HSA with different molar ratios of OA.** The HepG2 cells (5×10^5 cells/well) were first incubated with 5 μM DAF-FM DA for 1 h and then treated with 100 μM SNO-HSA with different amounts of bound OA in 10 mM phosphate-buffered saline, pH 7.4 in the dark at 37 °C. Some of the experiments with the highest OA concentration were also performed in the presence of 50 μM filipin III. Intracellular NO was monitored with DAF-FM fluorescence (ex/em of 385/535 nm). *Δfluorescence* represents DAF-FM fluorescence in cells incubated with different preparations of SNO-HSA, minus the fluorescence in cells that had been incubated with buffer only. Data are expressed as means ± S.E. ($n = 4$); the *bars* showing S.E. were smaller than the size of the symbols.

Fig. 9 proposes a model for *S*-transnitrosation from SNO-HSA. Binding of OA, or of a mixture of endogenous fatty acids, introduces conformational changes in SNO-HSA that render the *S*-nitroso moiety more accessible. OA binding also facilitates the binding of albumin to a receptor on the hepatocytes, perhaps the albumin binding adaptor protein gp60 (29). When bound to the receptor, SNO-HSA-OA can *S*-transnitrosate to HepG2 cells via two (or more) systems. Because OA-induced transnitrosation could be completely blocked by filipin III, an inhibitor of caveolae (19), it is proposed that caveolae are important for this type of *S*-transnitrosation. These findings strongly suggest that OA and NO of SNO-HSA-OA are transported by caveolae-associated proteins. Further studies are needed to identify and clarify the mechanism of the caveolae-associated proteins.

It is widely assumed that *S*-transnitrosation from SNO-HSA to cells takes place solely or mainly via low molecular weight thiols (6, 26, 30). In the present work, *S*-transnitrosation to HepG2 cells was studied in the absence of GSH and other low molecular weight thiols. In accordance with the assumption mentioned above, only a slight *S*-transnitrosation was detected

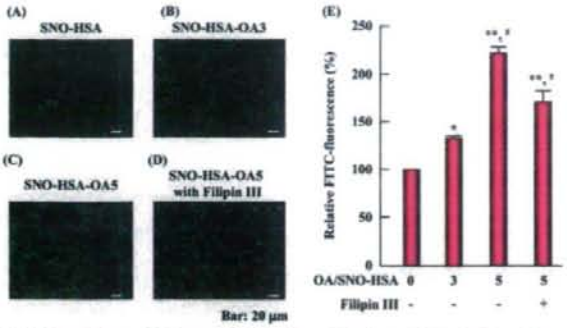

FIGURE 8. **Effect of OA and filipin III on binding of FITC-SNO-HSA to HepG2 cells.** To prepare FITC-SNO-HSA, HSA was first *S*-nitrosylated as described above, followed by FITC labeling. FITC-SNO-HSA (50 μg/ml) with varying OA content (0, 3, 5 OA/HSA) was dissolved in 10 mM phosphate-buffered saline (pH 7.4) and added to HepG2 cells (5×10^5 cells/well) for 10 min at 4 °C. In some experiments, the cells had been pretreated with 50 μM filipin III for 30 min. After incubation, the cells were washed twice with the phosphate-buffered saline to remove unbound FITC-SNO-HSA. After washing, the cells were analyzed using a fluorescence microscope. *E*, four columns quantify the FITC-fluorescence in *panels A, B, C,* and *D*, respectively, using the fluorescence in *panel A* as a reference value, *i.e.* 100%. The values are means ± S.E. ($n = 3$). *, $p < 0.05$ and **, $p < 0.01$, compared with the fluorescence of FITC-SNO-HSA without OA. #, $p < 0.05$, compared with the fluorescence of FITC-SNO-HSA with 3 mol of OA/HSA.

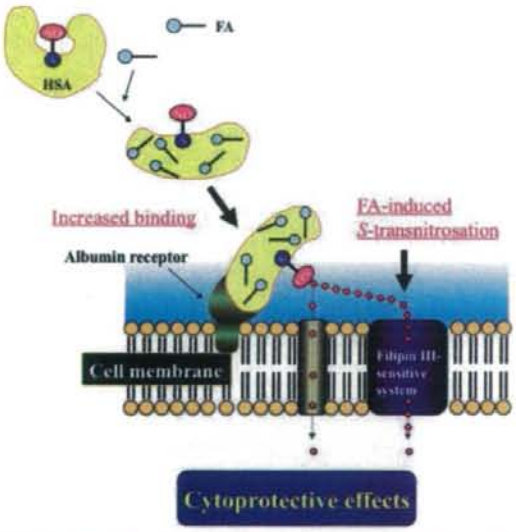

FIGURE 9. **Proposed model for the OA-mediated increase in *S*-transnitrosation of HepG2 cells by SNO-HSA.** The *S*-transnitrosation can lead to cytoprotective effects, see Figs. 1 and 2. *FA*, free fatty acid.

in the absence of OA. However, OA binding to SNO-HSA greatly increased the process.

In conclusion, fatty acid binding can improve the cytoprotective effect of SNO-HSA *in vivo*, and reinforcement of an antiapoptotic effect by fatty acid binding contributed to this result. Fatty acid bound to SNO-HSA can enhance the interaction between SNO-HSA and HepG2 cells, and the *S*-denitrosylation of SNO-HSA. This results in the enhancement of NO transfer from SNO-HSA into the hepatocytes, and to the antiapoptotic effect. Moreover, we found a novel filipin III-sensitive mechanism of the transfer of NO from SNO-HSA into the hepatocytes. Taken together, further study is now warranted to explore the roles of fatty acid binding in the pharmacological benefits of SNO-HSA, for which a clinical application is expected as a potent NO supplementary therapy.

Acknowledgments—We thank the members of the Gene Technology Center at Kumamoto University for important contributions to these experiments.

REFERENCES

1. Peters, T., Jr. (1996) *All About Albumin: Biochemistry, Genetics, and Medical Applications*, Academic Press, San Diego
2. Dworschak, M., Franz, M., Hallstrom, S., Semsroth, S., Gasser, H., Haisjackl, M., Podesser, B. K., and Malinski, T. (2004) *Pharmacology* **72,** 106–112
3. Hallstrom, S., Franz, M., Gasser, H., Vodrazka, M., Semsroth, S., Losert, U. M., Haisjackl, M., Podesser, B. K., and Malinski, T. (2008) *Cardiovasc. Res.* **77,** 506–514
4. Hallstrom, S., Gasser, H., Neumayer, C., Fugl, A., Nanobashvili, J., Jakubowski, A., Huk, I., Schlag, G., and Malinski, T. (2002) *Circulation* **105,** 3032–3038
5. Ishima, Y., Sawa, T., Kragh-Hansen, U., Miyamoto, Y., Matsushita, S., Akaike, T., and Otagiri, M. (2007) *J. Pharmacol. Exp. Ther.* **320,** 969–977
6. Crane, M. S., Ollosson, R., Moore, K. P., Rossi, A. G., and Megson, I. L. (2002) *J. Biol. Chem.* **277,** 46858–46863
7. Kragh-Hansen, U. (1981) *Pharmacol. Rev.* **33,** 17–53
8. Kragh-Hansen, U., Chuang, V. T. G., and Otagiri, M. (2002) *Biol. Pharm. Bull.* **25,** 695–704
9. Chen, R. F. (1967) *J. Biol. Chem.* **242,** 173–181
10. Akaike, T., Inoue, K., Okamoto, T., Nishino, H., Otagiri, M., Fujii, S., and Maeda, H. (1997) *J. Biochem. (Tokyo)* **122,** 459–466
11. Ikebe, N., Akaike, T., Miyamoto, Y., Hayashida, K., Yoshitake, J., Ogawa, M., and Maeda, H. (2000) *J. Pharmacol. Exp. Ther.* **295,** 904–911
12. Wang, X., Tanus-Santos, J. E., Reiter, C. D., Dejam, A., Shiva, S., Smith, R. D., Hogg, N., and Gladwin, M. T. (2004) *Proc. Natl. Acad. Sci. U. S. A* **101,** 11477–11482
13. Hnatowich, D. J., Layne, W. W., and Childs, R. L. (1982) *Int. J. Appl. Radiat. Isot.* **33,** 327–332
14. Yamasaki, Y., Sumimoto, K., Nishikawa, M., Yamashita, F., Yamaoka, K., Hashida, M., and Takakura, Y. (2002) *J. Pharmacol. Exp. Ther.* **301,** 467–477
15. Yamaoka, K., Tanigawara, Y., Nakagawa, T., and Uno, T. (1981) *J. Pharmacobiodyn.* **4,** 879–885
16. Gryzunov, Y. A., Arroyo, A., Vigne, J. L., Zhao, Q., Tyurin, V. A., Hubel, C. A., Gandley, R. E., Vladimirov, Y. A., Taylor, R. N., and Kagan, V. E. (2003) *Arch. Biochem. Biophys.* **413,** 53–66
17. Ishima, Y., Akaike, T., Kragh-Hansen, U., Hiroyama, S., Sawa, T., Maruyama, T., Kai, T., and Otagiri, M. (2007) *Biochem. Biophys. Res. Commun.* **364,** 790–795
18. Watanabe, H., Yamasaki, K., Kragh-Hansen, U., Tanase, S., Harada, K., Suenaga, A., and Otagiri, M. (2001) *Pharm. Res.* **18,** 1775–1781
19. Pohl, J., Ring, A., and Stremmel, W. (2002) *J. Lipid Res.* **43,** 1390–1399
20. Maeda, H., Ishida, N., Kawauchi, H., and Tuzimura, K. (1969) *J. Biochem. (Tokyo)* **65,** 777–783
21. Petitpas, I., Grune, T., Bhattacharya, A. A., and Curry, S. (2001) *J. Mol. Biol.* **314,** 955–960
22. Dasgupta, A., Kenny, M. A., and Ahmad, S. (1990) *Clin. Physiol. Biochem.* **8,** 238–243
23. Ristic, V., Tepsic, V., Ristic-Medic, D., Perunicic, G., Rasic, Z., Postic, M., Arsic, A., Blazencic-Mladenovic, V., and Ristic, G. (2006) *Ren. Fail.* **28,** 211–216
24. Stamler, J. S., Simon, D. I., Osborne, J. A., Mullins, M. E., Jaraki, O., Michel, T., Singel, D. J., and Loscalzo, J. (1992) *Proc. Natl. Acad. Sci. U. S. A* **89,** 444–448
25. Narazaki, R., Maruyama, T., and Otagiri, M. (1997) *Biochim. Biophys. Acta*

1338, 275–281
26. Shah, C. M., Bell, S. E., Locke, I. C., Chowdrey, H. S., and Gordge, M. P. (2007) *Nitric Oxide* **16,** 135–142
27. Stremmel, W., Pohl, L., Ring, A., and Herrmann, T. (2001) *Lipids* **36,** 981–989
28. Pohl, J., Ring, A., Ehehalt, R., Herrmann, T., and Stremmel, W. (2004) *Proc. Nutr. Soc.* **63,** 259–262
29. Minshall, A. D., Sessa, W. C., Stan, R. V., Anderson, R. G. W., and Malik, A. B. (2003) *Am. J. Physiol. Lung Cell Mol. Physiol.* **285,** 1179–1183
30. Simon, D. I., Stamler, J. S., Jaraki, O., Keaney, J. F., Osborne, J. A., Francis, S. A., Singel, D. J., and Loscalzo, J. (1993) *Arterioscler. Thromb.* **13,** 791–799

Biochimica et Biophysica Acta 1794 (2009) 634–641

Contents lists available at ScienceDirect

Biochimica et Biophysica Acta

journal homepage: www.elsevier.com/locate/bbapap

Altered chain-length and glycosylation modify the pharmacokinetics of human serum albumin

Yasunori Iwao [a], Mikako Hiraike [a], Ulrich Kragh-Hansen [b], Keiichi Kawai [c], Ayaka Suenaga [a], Toru Maruyama [a], Masaki Otagiri [a,*]

[a] Department of Biopharmaceutics, Graduate School of Pharmaceutical Sciences, Kumamoto University, 5-1 Oe-honmachi, Kumamoto 862-0973, Japan
[b] Department of Medical Biochemistry, University of Aarhus, DK-8000 Aarhus C, Denmark
[c] School of Health Sciences, Faculty of Medicine, Kanazawa University, Ishikawa 920-0942, Japan

ARTICLE INFO

Article history:
Received 19 September 2008
Accepted 3 November 2008
Available online 8 December 2008

Keywords:
Human serum albumin
Genetic variant
Pharmacokinetics
Half-life
Hepatic uptake
Renal disposition
Spleen uptake

ABSTRACT

Human serum albumin with modified plasma half-life will be useful for clinical purposes. Therefore, the pharmacokinetics of three of each of the following types of genetic variants, and of their corresponding normal albumin, were examined in mice: N-terminally elongated, C-terminally truncated and glycosylated albumins. Isoforms differing from the normal protein by three or more amino acids, especially two of the truncated forms, had shorter half-lives. The effect of glycosylation depended on the position of attachment: in domain II it increased half-life, whereas in domain I and III it had no significant effect. Liver, kidney and spleen uptake clearances were also modified. The pronounced changes in half-life of the two truncated variants and the glycosylated isoform could be explained, at least partly, by large changes in organ uptakes; in the remaining six cases, different effects were registered. Such information should be useful when designing therapeutical albumin products for, e.g., drug delivery systems. In addition to various types of cell endocytosis, leading to intracellular destruction or recycling of the proteins, the metabolism of the alloalbumins could be affected by plasma enzymes. No correlation was found between mutation-induced changes in the pharmacokinetic parameters and changes in α-helical content or changes in heat stability as represented by ΔH_v.

1. Introduction

Human serum albumin (HSA) is produced in the parenchymal cells of the liver, and it is the most abundant plasma protein. It is an important circulating depot protein and transport protein for endogenous and exogenous ligands in the blood, and contributes to the maintenance of osmotic pressure, plasma pH and to the Donnan-effect in the capillaries [1,2]. The protein is formed by a single polypeptide chain of 585 amino acids, and it has a molecular mass of approximately 66.5 kDa [2]. According to X-ray crystallographic analyses of HSA and of its recombinant version (rHSA), albumin has about 67% α-helix but no β-sheet. The analyses also showed that the polypeptide chain forms a heart-shaped protein with three homologous domains (I–III), each comprised of two subdomains (A and B) with distinct helical folding patterns that are connected by flexible loops [3,4]. A combined phosphorescence depolarization-hydrodynamic modeling study has proposed that the overall conformation of HSA in neutral solution is very similar to that observed in the crystal form [5].

Clinically, HSA is used for urgent restoration of blood volume, emergency treatment of chock, acute management of burns and other situations associated with hypoproteinemia [2]. To date, albumin has been produced by fractionation of whole blood. However, there is the potential risk of HSA contamination with blood-derived pathogens. In addition, human plasma can be in limited supply. Because of these problems, rHSA, which is highly expressed by *Pichia pastoris*, most probably will be commercially available in the near future [6]. Another benefit of this approach is that protein engineering will enable the creation of rHSAs with modified properties such as extended half-life in the circulation. In this connection HSA dimers seem to be useful candidates. Matsushita et al. [7] found that rHSA dimers had a high retention rate in the circulatory blood and a lower vascular permeability than native rHSA in normal rats and in mice with paw edema. Similar observations have been made by Komatsu et al. [8], who examined the pharmacokinetics of chemically crosslinked rHSA dimers in the rat. On the other hand, recombinant albumin domain(s) are cleared very fast. Sheffield et al. [9] found that recombinant domain I, I+II and III of rabbit serum albumin all had very short mean terminal catabolic half-lives in rabbits due to a fast elimination in the urine.

Abbreviations: HSA, human serum albumin; rHSA, recombinant HSA; Alb, albumin; Alb A, normal (wild-type) albumin; CD, circular dichroism; ΔH_v, van't Hoff enthalpy; RAGE, receptor for advanced glycation end products

* Corresponding author. Tel.: +81 96 371 4150; fax: +81 96 362 7690.
E-mail address: otagirim@gpo.kumamoto-u.ac.jp (M. Otagiri).

1570-9639/$ – see front matter © 2008 Elsevier B.V. All rights reserved.
doi:10.1016/j.bbapap.2008.11.022

Because of a relatively high in vivo half-life of ca. 19 days [2], HSA is an attractive fusion partner to extend the half-life, and potentially the therapeutic utility, of recombinant peptides and proteins. Among recent examples are rHSA genetically fused to type 1 interferons [10], glucagon-like peptide-1 [11] and interleukin-2 [12]. However, although an extension of the half-life of therapeutic peptides and proteins often is desirable, an extension to that of albumin could be excessive.

Although HSA-preparations with a modified half-life thus could be very useful, not much has been done to design or find such preparations. In our search for useful candidates, we have paid our attention to HSA genetic variants. Until now, 65 inherited variants of HSA, including proalbumin variants, have been identified and structurally characterized [13]. Usually, these genetic variants are expressed in heterozygous form and without any known association to disease [13]. Therefore, unlike lethal mutations, such may occur for hemoglobin and coagulation factors, studying the pharmacokinetic properties of HSA variants is a good way of gaining information which can be used when designing recombinant HSAs, because we can consider the effects of molecular variation without worrying about complications such as antigenic effects.

Recently, we have studied the pharmacokinetic properties in mice of 17 alloalbumins with single-residue mutations [14]. The study showed that, for example, only a few of the variants had a significantly modified half-life in the blood. In an attempt to find genetic variants with a more pronounced impact on pharmacokinetics, we now have expanded that study by determining the plasma half-lives and organ uptakes of three HSAs with a slightly longer chain-length (proalbumin variants), three with a slightly shorter chain-length (C-terminal variants) and three alloalbumins *N*-glycosylated in domain I, II and III, respectively. For being able to make a more detailed comparison between molecular characteristics and pharmacokinetic properties, we have estimated the effect of the molecular modifications on the α-helical content of the alloalbumins by using circular dichroism (CD). Previously, the effect of genetic variation on the thermal stability of HSA has been quantified in terms of, for example, changes in the van't Hoff enthalpy (ΔH_v) [15]. In the present work, the pharmacokinetic results have also been related to changes in ΔH_v.

2. Materials and methods

2.1. Protein samples

The genetic variants of HSA and their normal (wild-type) counterpart (endogenous Alb A) were isolated from serum from heterozygous carriers by ion-exchange chromatography. The locations of the structural changes of the nine variants are indicated in Fig. 1. After isolation, the albumins were checked for homogeneity by native electrophoresis, and no denaturation or significant (no more than 5%) cross-contamination between variant and Alb A was detected. The proteins were donated to us by Drs. M. Galliano and L. Minchiotti, University of Pavia, Pavia, Italy; Dr. S.O. Brennan, Canterbury Health Laboratories, Christchurch, New Zealand; and Dr. D. Donaldson, East Surrey Hospital, Redhill, UK. Before use, the albumins were delipidated by treatment with hydroxyalkoxypropyldextran at pH 3.0, as described in a previous paper [16]. After defatting, the albumins were dialysed extensively against deionized water, lyophilized and stored at −20 °C until used. Thus, the albumins from a donor have been exposed to exactly the same conditions from the time the blood samples were taken until the present experiments were performed.

Fraction V HSA (96% pure), assumed to be Alb A, was donated by the Chemo-Sera-Therapeutic Research Institute (Kumamoto, Japan) and defatted using the charcoal procedure described by Chen [17], deionized, freeze-dried and then stored at −20 °C until used.

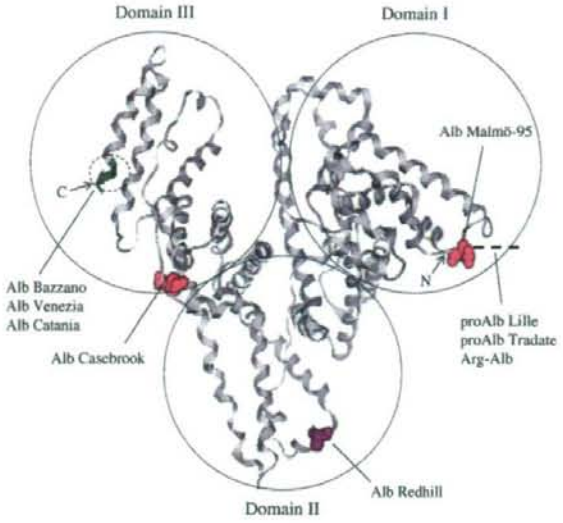

Fig. 1. The crystal structure of HSA indicating the locations of the mutations of the three C-terminal variants and the three proAlb variants used in this study. The locations of the glycosylated 63 Asn (Alb Malmö-95), 318 Asn (Alb Redhill) and 494 Asn (Alb Casebrook) are also shown. The subdivision of HSA into domains is marked; N and C stand for the N-terminal and the C-terminal ends, respectively. The broken, black line added to the N-terminal end indicates the prosegment of HSA.

2.2. Chemicals and animals

$^{111}InCl_3$ (74 Mbq/mL in 0.02 N HCl) was donated by Nihon Medi-Physics (Takarazuka, Japan). All chemicals were of the highest grade commercially available, and all solutions were prepared using deionized, distilled water.

Male ddY mice (26–32 g) were purchased from the Shizuoka Agricultural Cooperative Association for Laboratory Animals (Shizuoka, Japan), and were maintained under conventional housing conditions. All animal experiments were conducted in accordance with the principles and procedures outlined in the National Institute of Health Guide for the Care and Use of Laboratory Animals.

2.3. In vivo experiments

All proteins were radiolabeled with ^{111}In using the bifunctional chelating reagent DTPA anhydride according to the method of Hnatowich et al. [18], as described elsewhere [19]. In previous works, we found no significant differences in pharmacokinetic properties among these albumins, when ^{111}In-labeled mouse, rat, bovine or human serum albumin was administered to mice (unpublished), suggesting that immunogenic behavior does not occur in mice. Therefore, we chose the mouse as a reasonable model for the study of the pharmacokinetics of the HSAs. Mice received tail vein injections of ^{111}In-labeled proteins in saline, at a dose of 0.1 mg/kg and were housed in metabolic cages to allow the collection of urine samples. Urine samples were collected throughout the 120 min of the experimental period. In the early period after injection, the efflux of ^{111}In radioactivity from organs is assumed to be negligible, because the degradation products of ^{111}In-labeled proteins using DTPA anhydride cannot easily pass through biological membranes [20]. This assumption was supported by the fact that no ^{111}In was detectable in the urine after 120 min. At 1, 3, 5, 10, 30, 60, 90 or 120 min after injection, blood was collected from the vena cava under ether anesthesia and plasma was obtained by centrifugation. After blood collection, the animals were sacrificed, organs were excised, rinsed with saline and weighed.

The radioactivity of each blood and tissue sample was measured in a well-type NaI scintillation counter (ARC-500, Aloka, Tokyo).

Pharmacokinetic analyses were performed as follows. The plasma ^{111}In radioactivity concentrations (C_p) were normalized with respect to the percentage of injected dose and analyzed using the nonlinear least-square program MULTI [21]. The two-compartment model was fitted according to the Akaike information criterion by Eq. (1).

$$C_p = Ae^{-\alpha t} + Be^{-\beta t} \quad (1)$$

The half-lives of the HSAs were determined as β-phase elimination within a 120-min period. The tissue distribution patterns were evaluated using tissue uptake clearances (CL_{uptake}) according to the integration plot analysis. CL_{uptake} was calculated using Eq. (2).

$$CL_{uptake} = \frac{X_t/C_t}{AUC_{0-t}/C_t} \quad (2)$$

where X_t is the tissue accumulation at time t, AUC_{0-t} is the area under the plasma concentration time-curve from time 0 to t, and C_t is the plasma concentration at time t. CL_{uptake} was obtained from the slope of the plot of X_t/C_t versus AUC_{0-t}/C_t. We estimated the organ uptake clearances within a 30 min period.

2.4. Far-UV CD spectra

The protein concentration was 1.5 μM, as determined by the method of Bradford [22], and the buffer was 67 mM sodium phosphate, pH 7.4, 25 °C. Far-UV intrinsic spectra were recorded from 200 to 250 nm using a Jasco J-720 spectropolarimeter (Tokyo, Japan). For calculation of the mean residue ellipticity, $[\theta]$, the molecular masses were assumed to be 65.8 kDa for Alb Venezia, 67.1 kDa for proAlb Lille and Tradate and 66.5 kDa for the remaining variants and Alb A. The α-helical content of the proteins was estimated from the ellipticity values at 222 nm as described by Chen et al. [23].

2.5. Analysis of experimental data

The effects of the molecular changes were evaluated by using the following relationship:

$$\text{Percent change} = \frac{(\text{Result for variant}) - (\text{Result for Alb A})}{(\text{Result for Alb A})} \times 100\% \quad (3)$$

In Eq. (3), the result can be a value determined for plasma half-life, organ uptake clearance, α-helical content or for ΔH_v.

2.6. Statistical analysis

Statistical analyses were performed by using the Student t-test. A probability value of $P<0.05$ was considered to indicate statistical significance.

3. Results

3.1. The genetic variants

The alloalbumins used in this study have been named after the place from where the first detected carrier originates, and their molecular changes are summarized in Table 1.

Proalbumin (proAlb) is an albumin molecule to which the propeptide, Arg-Gly-Val-Phe-Arg-Arg-, is still bound at the N-terminus (Fig. 1). The positions of the propeptide are numbered from −6 to −1 (the juxtaposition to albumin). Normally, proAlb does not occur in detectable amounts in the circulation, because the propeptide is cleaved off by propeptidase within the liver cells. However, substitution of −1 Arg or −2 Arg (as in proAlb Lille [24] and proAlb Tradate [25]) inhibits the proteolytic cleavage of the propeptide but not the secretion of the protein, and such proalbumin variants, in contrast to wild-type proalbumin, can be isolated from the serum. In vivo, the prepro-form of proAlb Tradate (−2 Arg→Cys) is often cleaved after the mutated residue giving rise to HSA retaining −1 Arg (Arg-Alb) [25].

Among the C-terminal variants most are truncated albumins (Table 1). Thus, Alb Catania is three amino acids shorter than Alb A, and the three last residues in the new C-terminal end are changed from Gln-Ala-Ala to Lys-Leu-Pro [26]. Alb Venezia has been shortened by seven amino acids, and the new C-terminal end is changed from Gly-Lys-Lys-Leu-Val-Ala-Ala to Pro-Thr-Met-Arg-Ile-Arg-Glu [26]. Alb Bazzano has been shortened by three amino acids, and 14 of the last 16 amino acids in the new C-terminal end have been substituted: from Cys-Phe-Ala-Glu-Glu-Gly-Lys-Lys-Leu-Val-Ala-Ala-Ser-Gln-Ala-Ala to Ala-Leu-Pro-Arg-Arg-Val-Lys-Asn-Leu-Leu-Leu-Gln-Val-Lys-Leu-Pro [27]. Here the 567 Cys→Ala substitution has caused the loss of the C-terminal disulfide bridge.

It is uncommon for an amino acid substitution to result in the formation of an oligosaccharide attachment sequence. However, that has happened to Alb Malmö-95 [28], Alb Redhill [29,30] and Alb Casebrook [31,32], which are glycosylated in domain I, II and III, respectively (Fig. 1). In all three cases, the glycan is a disialylated (mainly or totally) biantennary complex type oligosaccharide N-linked to an asparagine residue [30]. Alb Redhill is unique, because it is

Table 1
Half-lives and organ uptake clearances of ^{111}In-labeled HSA variants and corresponding Alb A in mice

Variant name (mutation)	Domain		Half-life[a] (min)	Clearance (μL/hr)[a]		
				Liver	Kidney	Spleen
proAlb Lille (−2Arg->His)	I	Variant	251.1±4.31*	56.13±8.07	60.06±6.76	82.47±15.96
		Alb A	264.3±4.58	42.66±7.52	79.69±8.04	90.11±7.97
proAlb Tradate (−2Arg->Cys)	I	Variant	249.4±5.89	111.99±14.99	89.14±11.11**	74.83±13.57
		Alb A	252.4±7.62	109.99± 14.01	46.01±6.89	87.86±6.36
Arg-Alb (Alb A having −1 Arg)	I	Variant	262.1±6.53	21.16±3.72**	99.98±23.18	105.77±14.52
		Alb A	253.5±4.98	94.38±5.17	119.38±10.29	91.38±6.51
Alb Bazzano (567–582 substituted, 583–585 deleted)	III	Variant	231.1±5.31*	189.77±26.11**	253.69±36.22**	84.66±7.00**
		Alb A	245.2±6.93	41.35±4.68	119.95±20.05	57.94±5.11
Alb Venezia (572–578 substituted, 579–585 deleted)	III	Variant	225.1±5.49**	134.32±11.41**	136.11±13.55**	88.48±10.15
		Alb A	247.2±6.83	41.24±4.81	62.87±3.28	67.89±15.03
Alb Catania (580–582 substituted, 583–585 deleted)	III	Variant	248.6±5.46	12.29±1.18*	140.09±15.01**	45.97±5.15
		Alb A	251.3±3.99	48.99±18.18	81.53±12.02	52.69±7.64
Alb Malmö-95 (63 Asp->Asn, glycosylated at 63 Asn)	I	Variant	261.3±7.62	145.82±13.84**	113.96±15.72	53.21±4.21**
		Alb A	264.2±6.14	79.72±11.74	111.64±18.18	82.68±4.09
Alb Redhill (−1 Arg retained, 320 Ala->Thr, glycosylated at 318 Asn)	II	Variant	260.3±7.43*	25.69±3.51**	62.62±7.05**	45.68±6.91**
		Alb A	245.2±6.34	93.49±8.95	125.84±15.21	84.39±7.26
Alb Casebrook (494 Asp->Asn, glycosylated at 494 Asn)	III	Variant	251.2±4.88	134.79±13.97**	141.01±8.14	56.94±6.10
		Alb A	249.1±4.54	81.45±9.19	148.71±21.18	57.73±4.25

[a] The data are average values of 3–6 experiments (±SD). *$P<0.05$, **$P<0.01$ as compared with endogenous Alb A.

the only example so far of an albumin with two mutations. One is the 320 Ala→Thr, which leads to glycosylation of 318 Asn; the other is −2 Arg→Cys, which results in abnormal hydrolysis of the prepro-form within the liver cells and to the formation of albumin still possessing −1 Arg [29].

According to the literature cited [24–32], none of the mutations seem to affect the oligomeric state of albumin.

3.2. Pharmacokinetic properties of HSA variants

Fig. 2 shows the time courses for radioactivity in mouse plasma after intravenous administration of ^{111}In-labeled preparations of the variants and their corresponding Alb A. As seen, in all 9 cases the mutation affected, to different degrees, the elimination of HSA. Table 1 gives the plasma half-lives, calculated by β-phase using the nonlinear least-square program MULTI and Eq.(1), and liver, kidney and spleen uptake clearances, determined by an integration plot analysis (Eq.(2)). As a control we have compared the pharmacokinetic results obtained for endogenous Alb A (Table 1) with those obtained with commercial HSA (not illustrated), because both types of preparations are assumed to represent the normal protein. The average half-lives for Alb A and commercial HSA are 252.5 min and 268.2 ± 7.2 min (n = 6), respectively. The liver, kidney and spleen uptake clearances for Alb A are on an average 70.36 μL/h, 99.51 μL/h and 74.74 μL/h, respectively, whereas

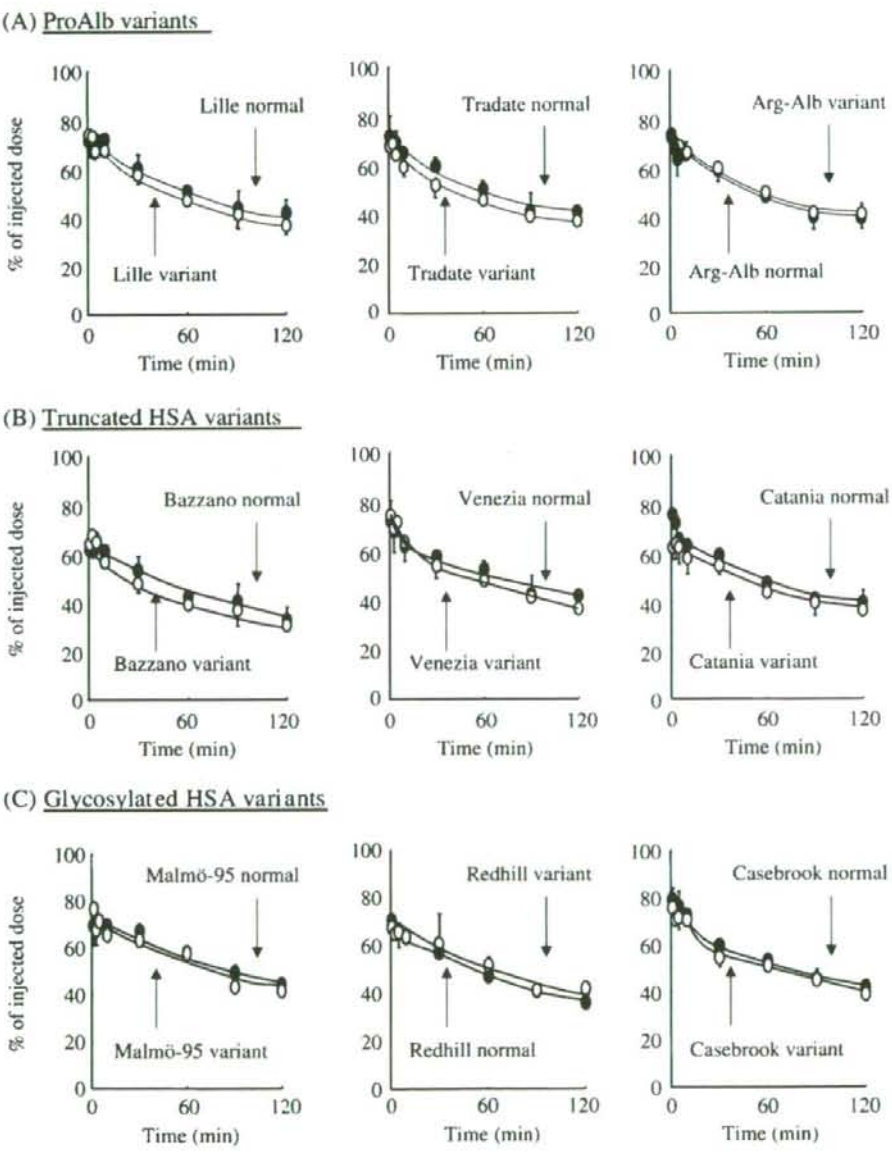

Fig. 2. Relative plasma amounts of ^{111}In-labeled proAlb variants (A), truncated HSA variants (B) and glycosylated HSA variants (C) and their corresponding Alb A after intravenous administration in mice. ^{111}In-albumin was injected as a bolus dose into the tail vein. Relative amounts are plotted against time after injection. The open and closed circles represent variant and normal albumin, respectively. Each point represents an average value obtained for 3–6 mice (±SD).